The NASA Seasonal-to-Interannual Prediction Project (NSIPP)

NASA/Goddard Space Flight Center

2001 Annual Report

August 22, 2002

The NASA Seasonal-to-Interannual Prediction Project (NSIPP) Annual Report for 2001

GOAL

To develop an assimilation and forecast system based on a coupled atmosphere-ocean-land-surface-sea-ice model capable of using a combination of satellite and in situ data sources to improve the prediction of ENSO and other major S-I signals and their global teleconnections.

OBJECTIVES

Demonstrate the utility of satellite data, especially surface height surface winds, air-sea fluxes and soil moisture, in a coupled model prediction system.

Aid in the design of the observing system for short-term climate prediction by conducting observation impact and predictability studies.

http://nsipp.gsfc.nasa.gov

Principal Investigator: Michele Rienecker, Code 971
Co-Investigators: Max Suarez, Code 913
David Adamec, Code 971
Randal Koster, Code 974
Siegfried Schubert, Code 910.3
James Hansen, Code 940

Funded by NASA/ESE: Global Modeling and Analysis Program
Physical Oceanography Research and Analysis Program

The NASA Seasonal-to-Interannual Prediction Project (NSIPP) Annual Report for 2001

Table of Contents

Summary Highlights

CGCM Simulations: Simulations have been conducted with the updated atmospheric model (NSIPP1 AGCM). Interannual variability is weak and biennial. Short simulations (5-10 years) were conducted to test the sensitivity of ocean SST to mixed layer parameters, the implementation of the surface mixed layer and to the eastern Pacific wind stress formulation.

Tier 1 Forecasts: Routine 12-month forecasts conducted monthly with 9-member ensembles.

Tier 2 Forecasts: Routine ensemble forecasts conducted monthly over Tier-1 forecast SST and IRI consensus SST forecast. The latter are contributed to IRI multi-model consensus forecast.

Predictability Studies: Nine 70-year AMIP-style simulations (1930-1999) have been conducted for use in predictability studies. Other predictability studies have focused on the impact of SST from different ocean basins on the atmospheric response during the 1982/83 and 1997/98 El Niño winters.

AGCM-LSM Experiments: Intermodel comparisons of the strength of land-atmosphere couplings included NSIPP, COLA, HadAM3 and CCM3 models. Intermodel differences appeared to result from differences in the treatment of boundary layer processes and moist convection. Analysis of soil moisture initialization and its impact on seasonal forecasts has continued using AMIP-style ensembles and forecast simulations. The extent to which the initialization improves forecasts is mixed.

Ocean Data Assimilation: The assimilation system has been updated to include the global subsurface temperature observations and to process data from the GODAE server in Monterey. A salinity adjustment scheme cross-validated with independent measurements in the equatorial Pacific has been shown to improve the temperature and zonal velocity estimates as well as salinity. The EnKF development has proceeded to include bias estimation and tests of altimetric data assimilation.

Land Data Assimilation: An ensemble Kalman Filter (EnKF) has been implemented for the land data assimilation system and compared with the extended Kalman Filter (EKF) developed by NSIPP science team members Jeff Walker and Paul Houser. The EnKF performs as well as the EKF with only 4 ensemble members and can account for a wider range of model errors. The EnKF thus appears to be a more promising approach to soil moisture initialization.

AGCM development: Development has proceeded with the NSIPP2 AGCM which includes a prognostic cloud condensate scheme as well as a shallow convection/PBL entrainment parameterization scheme. Comparisons with ISCCP observations are encouraging. In addition, parameter sweeps were undertaken in the NSIPP1 AGCM to identify factors controlling the formation of double ITCZs. Highly efficient convective precipitation (i.e., rapid auto conversion and weak rain re-evaporation) exhibits a pronounced double ITCZ while low efficiency produces a single ITCZ.

LSM development: Tests of the catchment model have continued as part of PILPS-2E. Other developments have focused on the improvement of run off generation through improved treatments of storm flow and base flow.

AGCM Simulations: Simulations at 0.5 degree resolution have been initiated. The first experiments were short simulations of the 1997/98 El Niño and 1998 La Niña. Water vapor distributions were realistic. These simulations were conducted to demonstrate the feasibility of conducting global simulations at the resolution often used for regional climate models.

Background

Understanding and predicting seasonal-to-interannual climate variations is a primary goal within NASA's climate research. The NASA Seasonal to Interannual Prediction Project (NSIPP) has been established as a core research and development activity at the Goddard Space Flight Center (GSFC) to develop the use of existing and planned remote observing systems together with in situ observations for experimental predictions of seasonal-to-interannual climate variations. By focusing on the application of remotely sensed observations, NASA expects to make unique contributions to the USGCRP, CLIVAR and GEWEX international research programs.

The NSIPP approach is based on the premise that coupled ocean-atmosphere-land general circulation models (CGCMs) offer the best prospect for predicting tropical sea surface temperature (SST) anomalies and of extending the prediction of global precipitation and temperature anomalies. The NSIPP CGCM is comprised of the NSIPP1 atmospheric model, the Poseidon quasi-isopycnal ocean model and the Mosaic land surface model (LSM). Coupled simulations are run routinely at 2 degrees for the atmosphere and 1/3 degree for the ocean. Finer resolution AGCM simulations, both 0.5 and 1 degree, are being run experimentally.

NSIPP produces routine experimental ENSO predictions of SST for the tropical Pacific region by assimilating subsurface temperature observations. The SST from these predictions is used to force coupled atmosphere-land (Tier 2) ensemble predictions. Ensembles allow the characterization of the uncertainty of the forecasts. Categorical Tier 2 forecasts are presented on the world wide web.

Developments in ocean data assimilation to improve the characterization of model background errors have been a focus for NSIPP. In particular, we have undertaken the development and implementation of multivariate techniques needed when only subsurface temperature and/or surface height observations are available. In the coming year we will include the T-S correction scheme and sea surface height observations in the initialization of the coupled forecasts. Tests of the ensemble Kalman filter with the global model will be conducted.

Land data assimilation has also been one of NSIPP's priorities and for this we have maintained a close collaboration with our science team. In the coming year we will begin testing the impact of land surface initialization on Tier 2 forecasts.

NSIPP will continue to examine the predictability of El Niño and other major climate variations on seasonal-to-interannual time scales and the predictability of extra-tropical signals. During the year we have begun two collaborations of special note: participation in the Earth System Modeling Framework (ESMF) consortium, and participation as a NOAA/OGP/CDEP Applied Research Center (ARC) to contribute to IRI and NOAA/NCEP/CPC operational forecasts.

Summary of Activities, January 2001 – January 2002

1. CGCM Experiments

CGCM experiments have been conducted to explore the dependence of coupled model SST biases on ocean model parameters (penetrating short wave radiation, mixed layer parameters, vertical mixing) and on the coupling in the eastern equatorial Pacific. Cold biases in the subtropical and midlatitude SST led us to test the sensitivity both to artificial low level cloud (fog) and to the floor value used to calculate evaporation. However, we were not able to reduce the bias, but rather found a large sensitivity to some of the constraints imposed on mixed layer entrainment. This led us to reformulate the representation of the mixed layer in the model. Instead of defining the topmost layer of the model to be the mixed layer, the mixed layer depth (MLD) was diagnosed from a Sterl and Kattenberg (1994) implementation of the Kraus-Turner formulation and then used merely to define the depth over which enhanced mixing was imposed. Forced ocean simulations were used to assess the model performance in terms of MLD and near-surface ocean structure composed with ocean surveys. A multi-decade coupled simulation has been re-initiated in early 2002.

2. Forecasts

2.1 Tier-1 forecasting system for 2001-2002

During 2001, the tropical Pacific surface temperatures were colder than normal in the east and warmer than normal in the west and central Pacific, especially after May 2001. This cold ENSO signal was associated with an intensified mean Walker circulation with a negative annual mean zonal wind stress anomaly on the equator from 170E to 80W. Annual mean wind stress was near normal from 140E to 170E. However, strong westerly wind bursts occurred over the western Pacific after May 2001 compensating for the stronger than normal easterlies observed before May 2001. The strongest of these bursts was observed in December 2001.

These wind bursts were accompanied by weak warm Kelvin waves that were not able to affect the eastern Pacific surface until the December event. When subsurface temperature anomalies in the western and central Pacific were as large as 6°C. These anomalies propagated eastward. A similar subsurface evolution was observed in 1991-1992 without a significant ENSO event and in 1997-1998 El Niño with a major ENSO event.

The 2001 ENSO forecasts with the NSIPP v0 system were consistently calling for a weak warming of the eastern Pacific that never occurred (Figure 2.1). This behavior can be attributed to a warm subsurface temperature anomaly in the western Pacific present in the initial conditions. The model propagated this anomaly eastward with a decreasing amplitude.

The NSIPP v0 forecasting system (with latest initialization for this report being January 2002) suggests that no ENSO event will occur during 2002. This evolution is based on the formation of negative subsurface anomalies that result in a premature end to the El Niño evolution as was observed during 1991-1992.

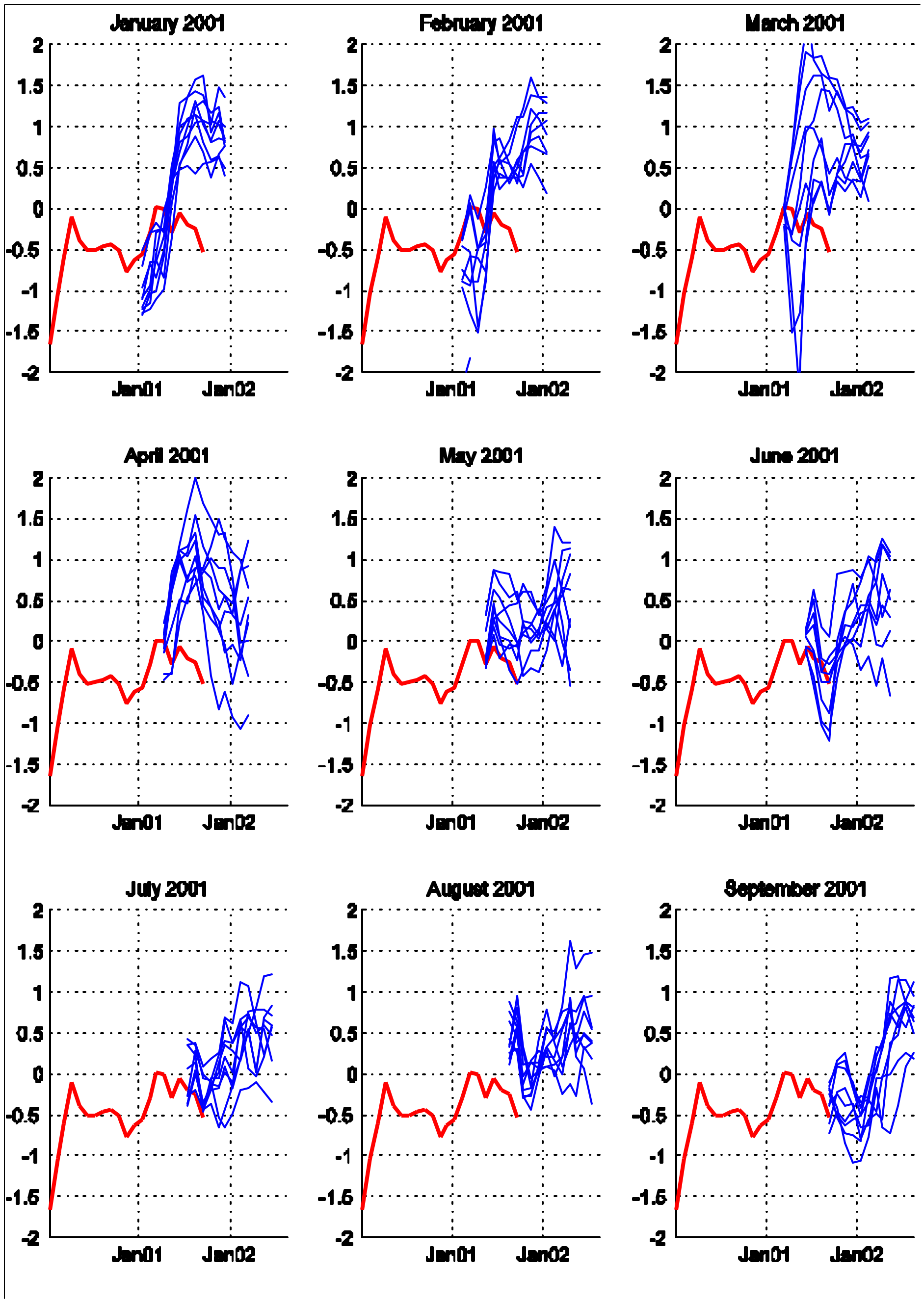

Figure 2.1 Ensemble forecast of Niño 3 averaged temperature anomalies (blue thin lines) versus the observed anomalies for year 2001.

2.2 Analysis of the CGCM v0 Forecast System (Tier 1)

The optimal configuration for an ENSO forecasting system is a good model of the phenomenon itself and a realistic forecast initialization. How good a model it has to be and how close to reality it has to be initialized is still unknown. Currently, the weakest aspect of ENSO forecasting with coupled general circulation models seems to be the inadequate representation of the phenomenon itself. Most coupled models, when allowed to evolve freely for decades, show a weaker ENSO signal with shorter time scales than observed. In fact, in many cases not only the interannual variability but also the mean climate and annual cycle are deficient.

The CGCM v0 underestimates both amplitude and extent of SST anomalies along the equator (Figure 2.2). The weakness of the simulated surface ENSO signal is related to a weak signal subsurface (Figure 2.3). For both observations and simulation the maximum subsurface temperature variability is found in the mean thermocline, but the amplitude of simulated anomalies is about half that of observations. The two first EOFs of subsurface temperature anomalies describe the role of the ocean during evolution of an ENSO event. The second EOF leads the first by 9 months for observations and 7 months for the model. Temperature anomalies first appear in the western Pacific at the level of the mean thermocline and then propagate eastward towards the eastern Pacific surface following a path defined by the mean thermocline. The faster timescale for the transition between EOF2 to EOF1 of the simulated temperature anomalies indicates a shorter mean periodicity for modeled ENSO events. Indeed, the dominant timescale for the model ENSO is quasi-biennial in the CGCMv0. It is worth noticing that the model signal in the western Pacific is much weaker than observations. This is perhaps due to a weaker atmospheric forcing resulting from the weaker SST anomalies in the eastern Pacific. Such a bias should not be very important for ENSO forecasts because data assimilation initializes the western Pacific with the correct temperature anomaly. However, if the amplitude of this signal cannot be maintained while it propagates eastward then the negative impact on a forecast is clear.

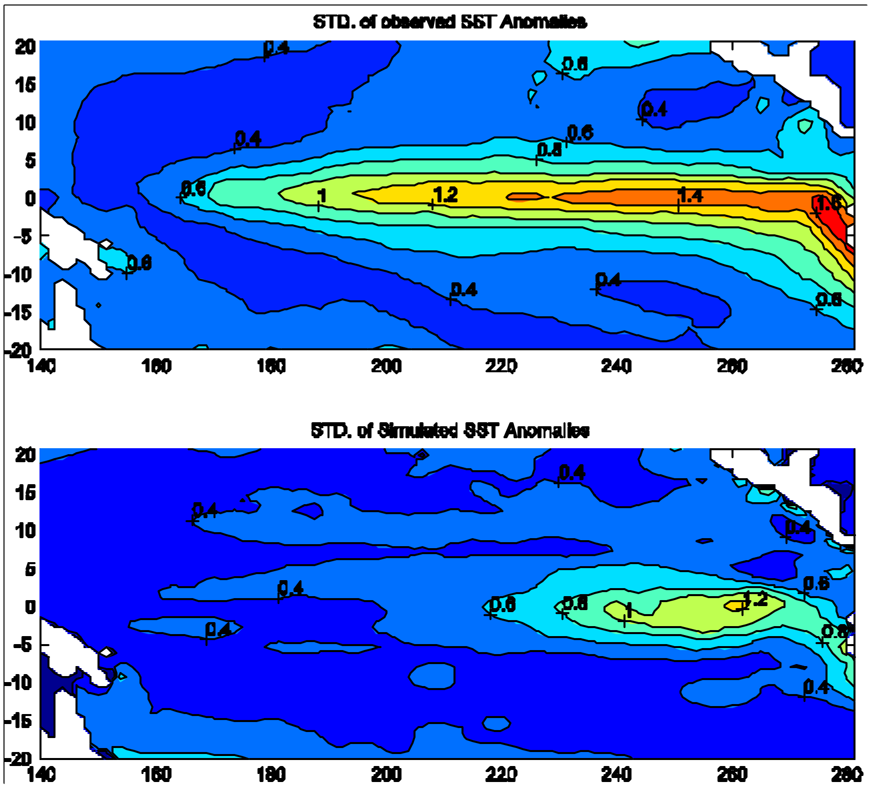

Figure 2.2 Standard deviation of Sea Surface Temperature anomalies. The upper panel is computed using the Reynolds observations, the lower from NSIPP's CGCMv0.

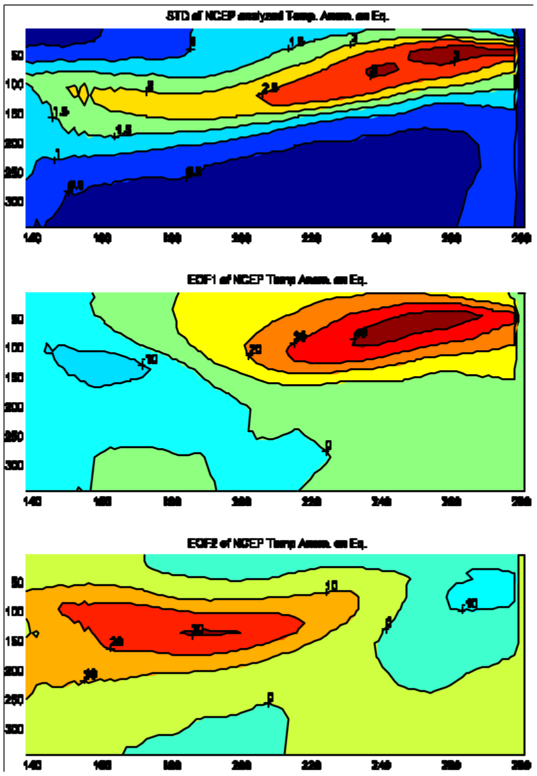

Figure 2.3a Top panel: standard deviation of temperature anomalies along the equatorial longitude vs. depth plane, Middle panel: first EOF of temperature anomalies along the equatorial longitude vs. depth plane and Bottom panel: second EOF. The NCEP ocean analysis.

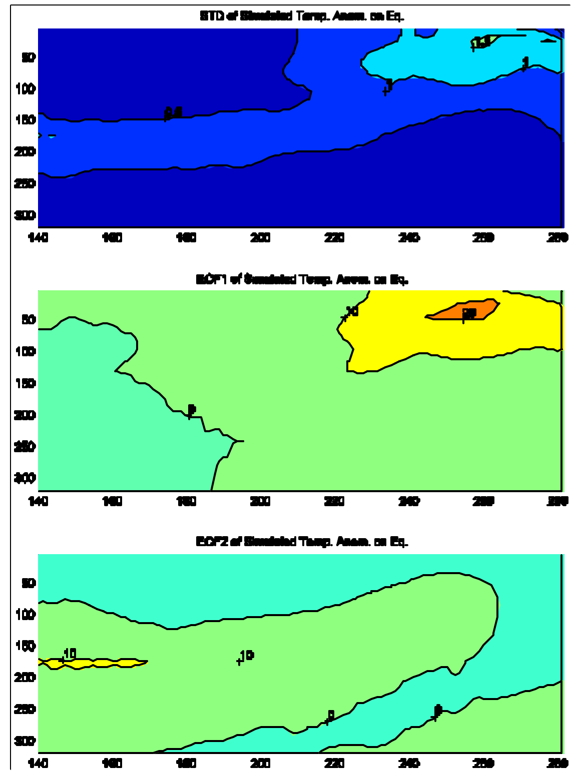

Figure 2.3b Same as Figure 2.3a for the NSIPP CGCMv0 simulated temperature field.

Review of the adjustment to the free coupled climate and of the forecast performance.

The current initialization procedure of the NSIPP forecast initiates two, possibly interacting adjustments. First, the ocean model adjusts from its initial state, which contains information from the real world, towards its own dynamical representation of this world. This adjustment can be defined by an experiment where the ocean model evolves in forced mode from an assimilated initial state. Secondly, when the atmospheric and ocean models are coupled, errors in boundary layer representation play a significant role in producing an unrealistic mean climate and variability. We have shown previously that initialization of the ocean state by assimilating TAO temperature increases the prediction skill of interannual SST anomalies. To compensate for the coupled adjustment (drift), the anomalies are defined as departures from the mean drifting forecast (annual cycle and mean state) as proposed by Stockdale (1997).

The evolution of the mean Niño 3 average SST and the evolution of the standard deviation of anomalous SST as a function of forecast lead time are presented in Figures 2.4a and 2.4b respectively. The mean Niño 3 SST of the coupled model is almost identical to the observed for the first month after initialization. It then undergoes a rapid cooling until the 6^{th} month after which it remains constant. Further evolution of this quantity is expected as the mean Niño 3 SST of the free coupled model is 26 degrees Celsius i.e., very close to the observed value (Reynolds and Smith, 1995). Figure 2.4b shows that the standard deviation for each month after initialization is initially stronger than observations but then drops rapidly reaching the level found in the free coupled model at about 7 months after initialization. Thus the mechanisms responsible for weak SST anomalies in the free coupled model act on short time scales.

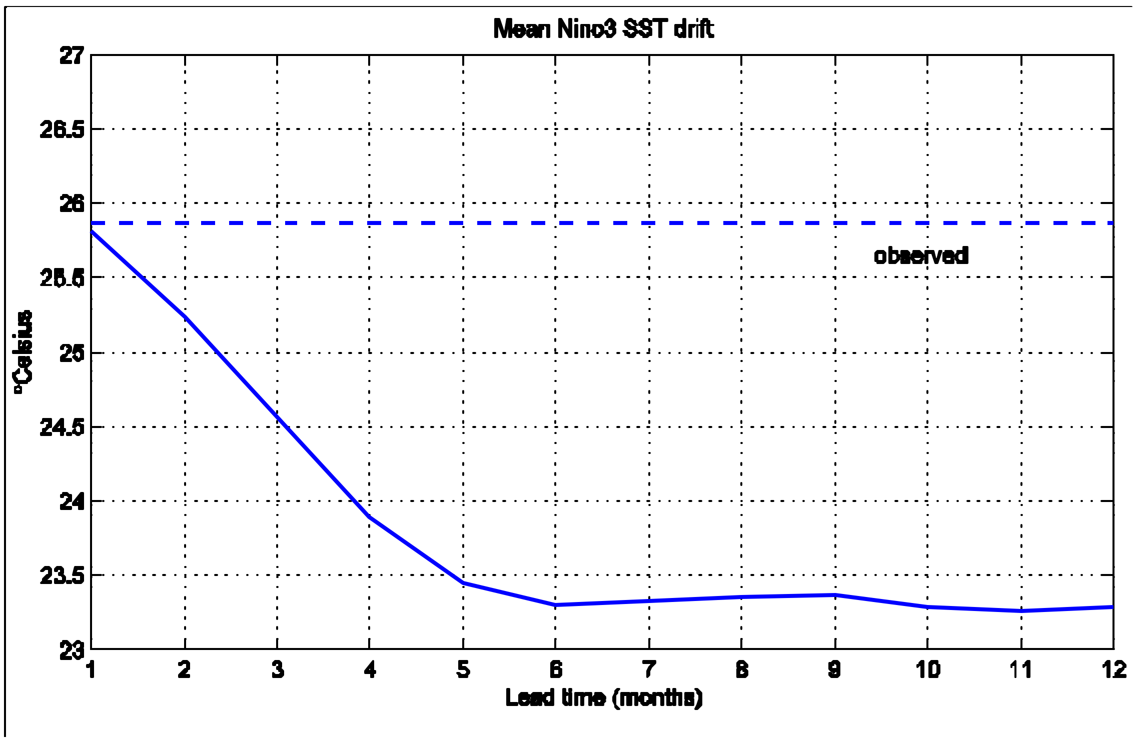

Figure 2.4a Evolution of the mean annual SST average over the Niño 3 area as a function of lead time from initialization.

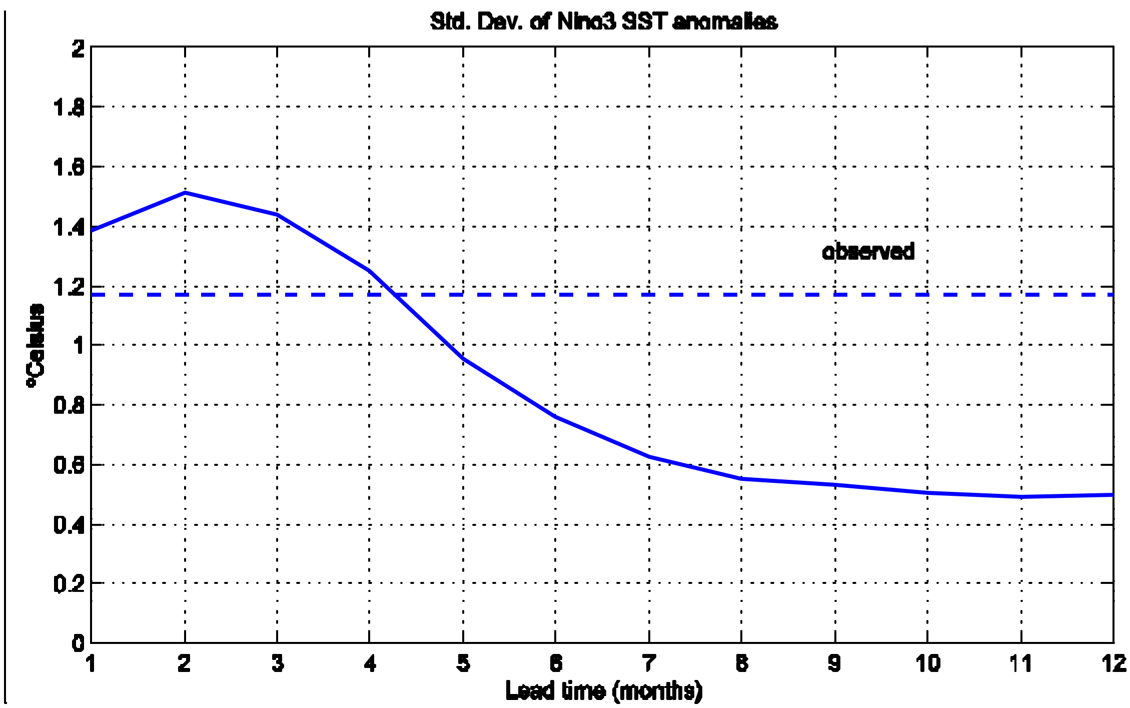

Figure 2.4b As for 2.4a, but for the standard deviation of temperature anomalies averaged over the Niño 3 area.

2.3 AGCM-LSM (Tier 2) Forecasts

Two sets of Tier 2 forecasts are produced routinely every month and posted at http://nsipp.gsfc.nasa.gov. Each is an ensemble of four-month runs of the atmosphere-land model using prescribed, forecast SSTs. The two sets are conducted with NSIPP and NCEP Tier 1 forecast SST respectively. The latter set is comprised of 9 ensemble members and are contributed to the IRI multi-model consensus forecast.

3. Predictability Studies

3.1 Tier 2 Predictability with the NSIPP AGCM

Our focus this year has been on the analysis of a number of long AMIP-style runs. These consist of nine 70-year simulations (1930-1999) forced with observed sea surface temperatures. We have also carried out several simulations with idealized SST. These consist of runs with perpetual ENSO warm or cold conditions (to examine the non-linearity of the response to ENSO), and runs forced with the 2 polarities of the dominant low frequency (> 6years) pattern of SST variability (Figure 3.1). The latter is a pan-Pacific anomaly pattern that appears to play an important role in the development of long term drought in the United States Great Plains.

We have continued our analysis of northern winter variability, focused on distinguishing between the variability that is forced by the SST and that variability that is internal (or free) to the atmosphere. We showed that rotated EOFs are a useful tool in that regard, and should help to better isolate the forced variability in the observations, especially on monthly time scales.

We have also carried out a detailed analysis of the nature of the differences in the atmospheric anomalies during the 1982/83 and 1997/98 El Niño winters. A large number of simulations were carried out with SST anomalies confined to different ocean basins to help clarify the importance of the SST in different locations as well as to determine the importance of the memory of the initial atmospheric conditions.

3.2 Predictability: Comparisons With Other AGCMs

An on-going collaboration with Arun Kumar at the National Centers for Environmental Prediction (NCEP) centers on the northern summer seasonal prediction problem. Our current work compares the predictability of the zonally-symmetric and asymmetric components of the flow during summer and winter in both the NCEP and NSIPP models. The results highlight the importance of the zonally symmetric flow during the northern summer.

A collaboration with David Straus of COLA involves a comparison of several different models (NSIPP, NCEP and COLA) with a focus on the variability and predictability of seasonal means during the transition seasons. The analysis attempts to extract the variability that is most predictable based on a method that maximizes the signal to noise ratio. The results show rather striking differences between the spring and fall seasons.

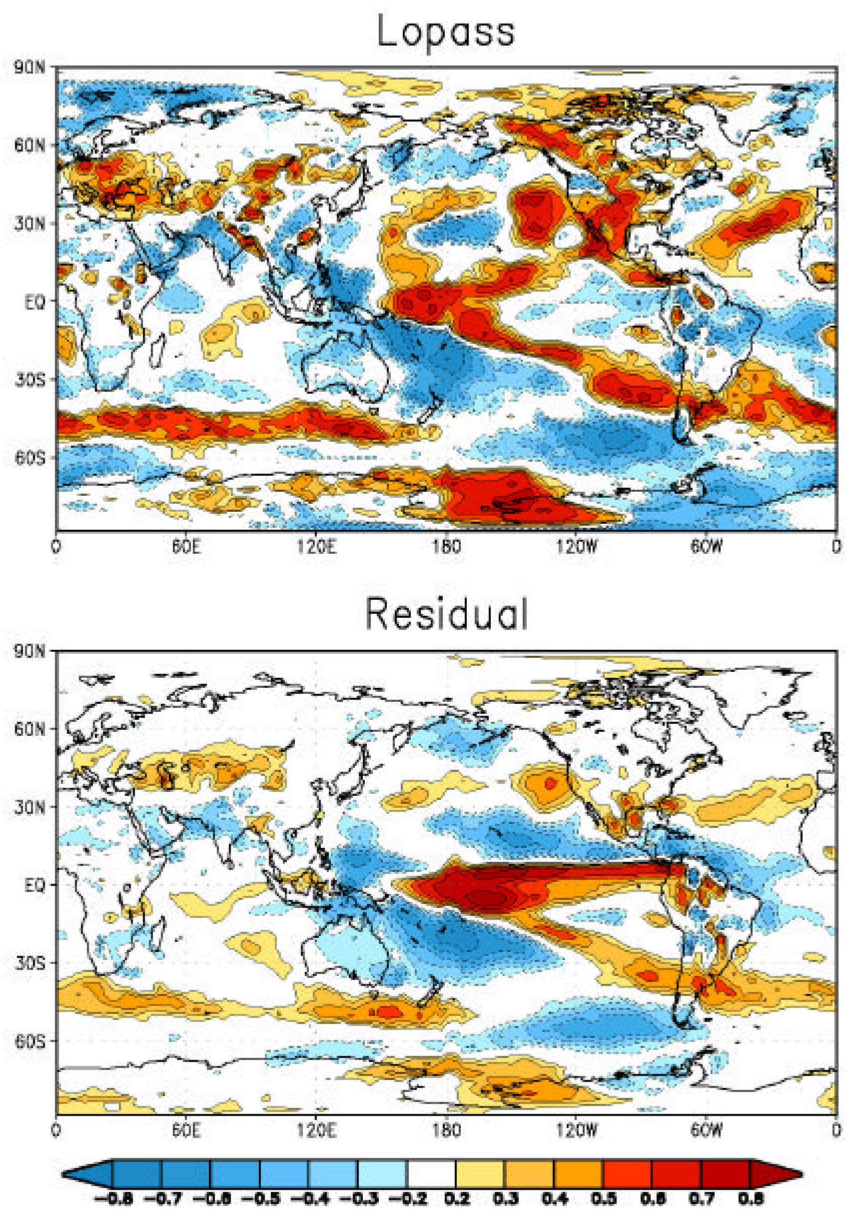

Figure 3.1 Top panel: The correlation between the leading low frequency (time scales longer than 6 years) pan Pacific SST principal component (PC) and the low frequency ensemble mean precipitation for the period 1930-1999. Bottom panel: Same as the top panel, except for the ENSO SST PC computed from the residual (total-low frequency) SST fields.

4. Coupled AGCM-LSM Experiments

Our studies of land-atmosphere interaction have progressed substantially this last year, as indicated by the following summary.

a. Soil moisture memory. The paper describing our work on what controls soil moisture memory (summarized in last year's report) has been revised and is now published (Koster and Suarez, 2001).

b. Our intermodel comparison of the strength of land-atmosphere coupling (introduced in last year's report) has been extended to four models, and a paper describing the results has been accepted for publication in the Journal of Hydrometeorology (Koster et al., 2002). The main result of the study is shown in Figure 4.1. Plotted for each of the four models is the global field of a derived coupling index that varies from zero, signifying no coupling strength, to one, signifying a very high coupling strength. The NSIPP model appears to have the highest coupling strength of the four. The study does not attempt to evaluate the relative realism of the models, since real-world values of coupling strength are unknown; rather, the idea is to present the intermodel differences as an indication of current uncertainty associated with the modeling of coupled processes. The intermodel differences appear to result from differences in the treatment of boundary layer processes and moist convection.

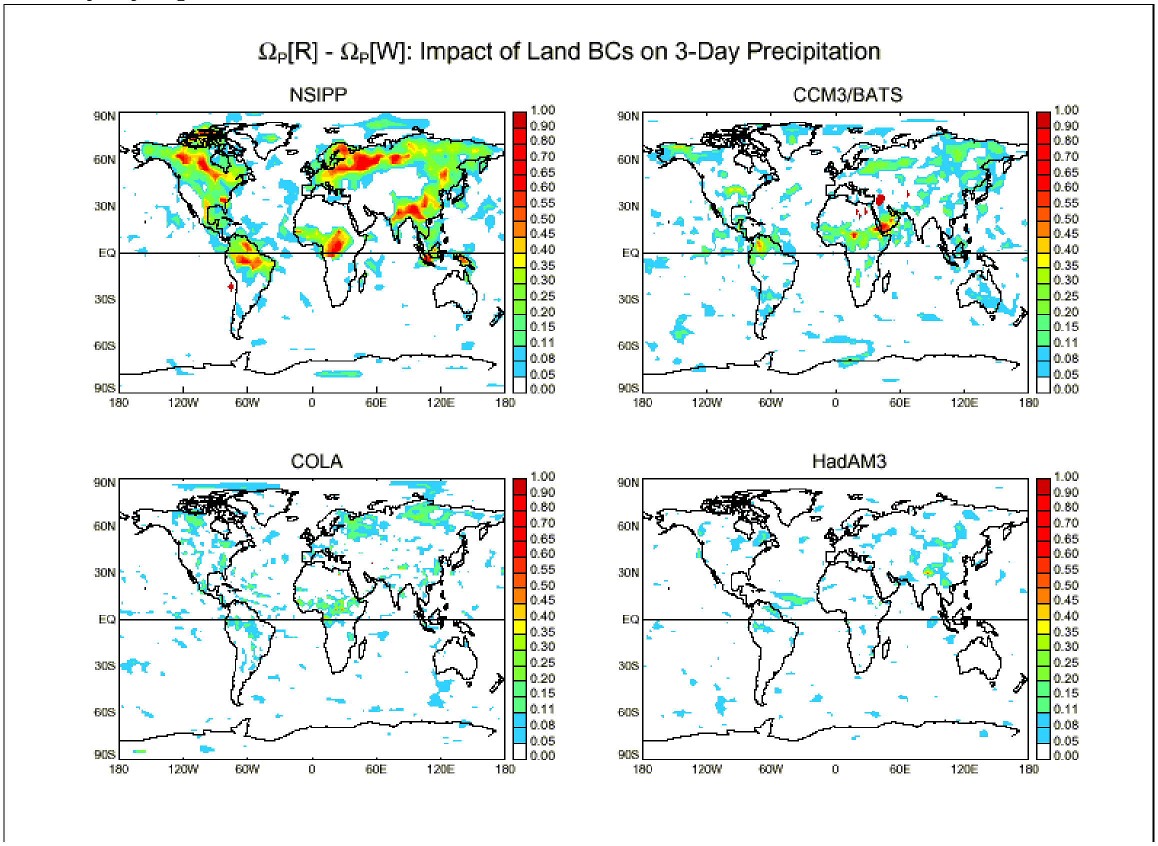

Figure 4.1 The degree to which precipitation generation is tied to surface conditions for four different GCMs. To produce the plot, each modeling group generated an ensemble of one-month July simulations, with each ensemble member forced to maintain the same (spatially-varying) time series of land surface states. The coupling index is related to the degree of coherence in the precipitation signal amongst the ensemble members. (Ocean effects are subtracted out via supplemental ensembles.)

c. The main focus of our work in 2001 has been the analysis of soil moisture initialization in the NSIPP Tier 2 system and its impact on seasonal forecasts. For each boreal summer during 1997-2001, we generated two 16-member ensembles of 3-month simulations. The first, "AMIP-style", ensemble establishes the degree to which a perfect prediction of SSTs would contribute to the seasonal prediction of precipitation and temperature over continents. The second ensemble is identical to the first, except that the land surface is also initialized with "realistic" soil moisture contents through the continuous prior application (within GCM simulations leading up to the start of the forecast period) of a daily observational precipitation data set. A comparison of the two ensembles shows that soil moisture initialization has a statistically significant impact on summertime precipitation and temperature over a handful of continental regions, as indicated in Figure 4.2. Furthermore, our analysis shows that these locations could have been predicted ahead of time by diagnostically identifying regions with (1) a tendency toward large initial soil moisture anomalies, (2) a strong sensitivity of evaporation to soil moisture, and (3) a strong sensitivity of precipitation to evaporation (Figure 4.3). This approach to identifying regions of impact prior to making forecasts may have relevance to other forecasting systems. The extent to which the initialization actually improves the forecast is mixed; improvement is seen in some years but not in others. The focus of research in 2002 will be a thorough investigation of this mixed performance.

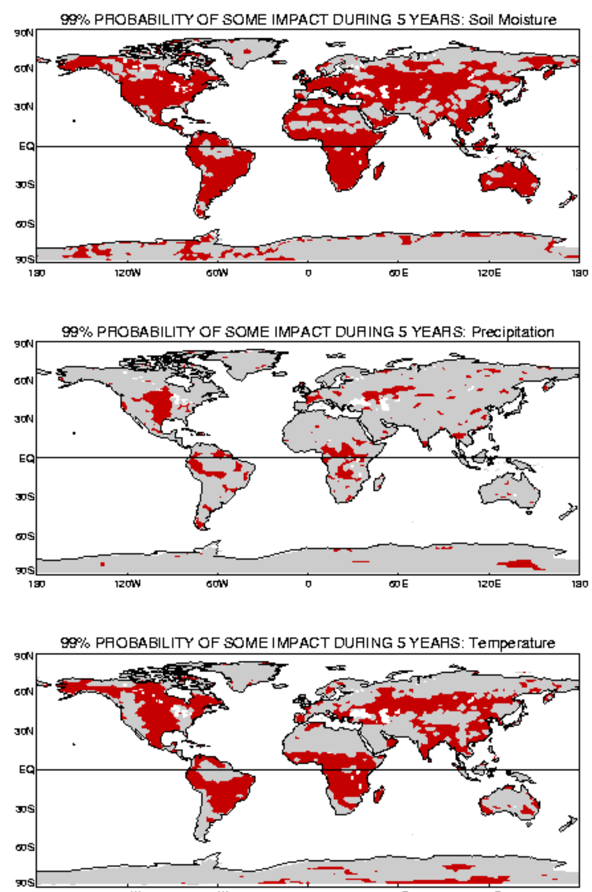

Figure 4.2 Composite maps showing the locations where, in a series of ensemble forecast experiments, June 1 soil moisture initialization had a significant impact, at least once during the 5 years studied, on JJA soil moisture (top), JJA precipitation (middle), and JJA surface temperature (bottom). Significance is at the 99% level.

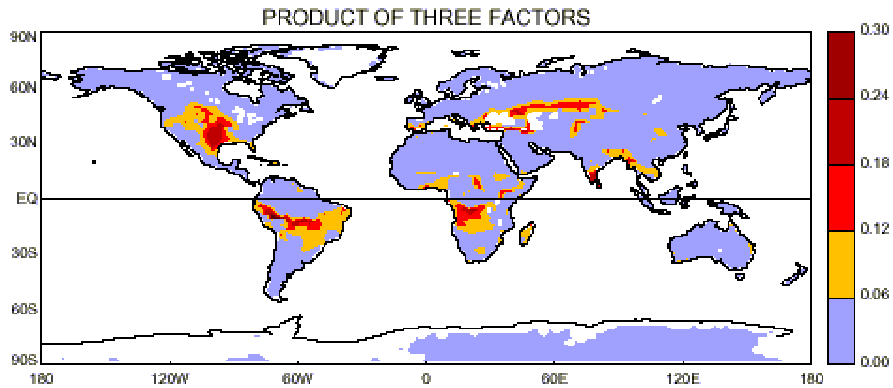

Figure 4.3 Product of three quantities related to soil moisture's impact on precipitation: (1) characteristic size of initial soil moisture anomaly, as measured by the standard deviation of total June 1 soil water (in units of degree of saturation); (2) slope of the evaporation ratio versus soil moisture relationship; and (3) convective fraction. Because all three quantities must be large for soil moisture initialization to affect subsequent precipitation, their product is a crude measure of the potential for such an impact. The locations where the product is large do, in fact, agree with the patterns shown in the middle plot of Figure 4.2.

d. Research into the impacts of interannually varying vegetation phenology, described in last year's report, has been completed, and a paper describing the results has been submitted to the Journal of Hydrometeorology (Guillevic et al., 2002).

5. Ocean Data Assimilation

5.1 A Hierarchy of Systems

NSIPP is currently testing three ocean data assimilation systems (ODAS), each with increasing degrees of sophistication in the sequential estimation hierarchy. The three systems are univariate optimal interpolation (UOI), multivariate optimal interpolation (MvOI), and the ensemble Kalman filter (EnKF). For the UOI, only temperature data are assimilated and only temperature is corrected directly by the assimilation procedure. For the MvOI, all components of the ocean state (temperature, salinity, currents, sea surface height) are corrected directly by the assimilation even if a single variable, such as temperature or sea surface height, is assimilated. For the MvOI, the error statistics, both level of error variance and structure of covariances, remain fixed throughout the assimilation cycle. The error statistics for the MvOI have been estimated from a single snapshot of an ensemble of ocean runs. In contrast, the EnKF uses the evolving spread of an ensemble of ocean states to estimate the evolving multivariate error statistics.

5.2 Univariate Optimal Interpolation – Correcting Salinity

Assimilation of temperature data has improved the quality of ocean state estimates used to initialize the coupled model forecasts conducted by NSIPP. Nonetheless, deficiencies in the density field are still present. One of the main reasons for such deficiencies is related to the fact that salinity is not analyzed and its effect on the density field is not negligible. We have implemented the scheme of Troccoli and Haines (1999, hereafter TH99) to correct salinity even though only temperature observations are assimilated. Salinity increments are derived from a scheme that uses the analyzed temperature along with the model temperature and salinity to preserve the model's water masses.

The scheme was cross validated with independent measurements of temperature, salinity and zonal velocity from TAO servicing cruises (Johnson et al, 2000). Two experiments were performed: a) only temperature updated (TOI) and b) both salinity and temperature updated (TOIS) with salinity increments given by the TH99 salinity scheme. For reference, a third run with no data assimilation (CNT) was conducted. The effectiveness of the salinity scheme is reflected not only in a better salinity field but also in improved zonal velocity and temperature fields. In particular, a root-mean-square difference (RMSD) analysis with respect to observations in the Niño4 and Niño3 regions shows an average improvement, of TOIS with respect to TOI, of 57% in the salinity field and of 32% in the temperature field in the upper 900m (Figure 5.1a-d). Also, the zonal velocity field is improved by an average of 17.5% in the upper 450m where observations are available (Figure 5.1e-f). The scheme is now being used for global assimilation of all available temperature profiles.

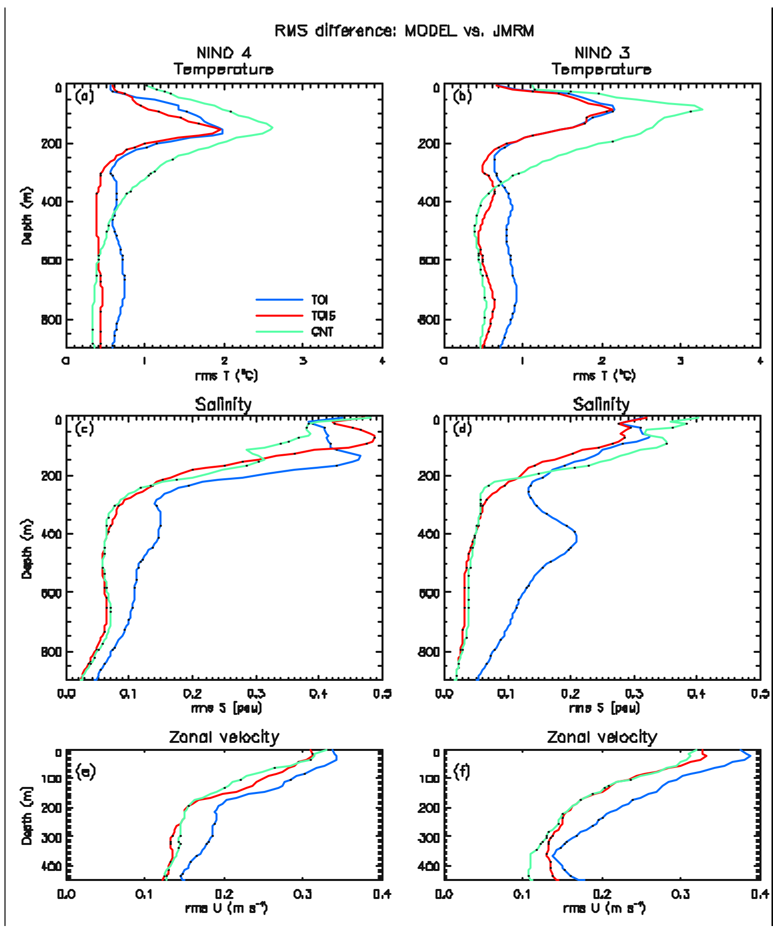

Figure 5.1 RMSD between the three model runs (TOI, TOIS and CNT) and observations as a function of depth for the 35 transects analyzed by (Johnson et al, 2000) grouped in Niño4 (a,c,e) and Niño3 (b,d,f). Temperature RMSD (a-b), salinity RMSD (c-d) and zonal velocity RMSD (e-f).

5.3 MVOI – Validation and tests of the robustness of the covariance estimates

We have estimated model forecast error statistics by Monte-Carlo techniques from an ensemble of model integrations generated by forcing the ocean model with an ensemble of air-sea fluxes. An important advantage of using an ensemble of ocean states is that it provides a natural way to estimate cross-covariances between the fields in the context of the governing dynamical balances. This initial implementation attributes all of the ocean model forecast error to uncertainties in the longer time scale surface flux anomalies, since differences between the ensemble members were due to atmospheric internal variability.

A cross-validation was conducted for the MvOI as for the UOI. Results were broken down by hemisphere since the salinity structures are different on either side of the equator. From the RMS errors between the model runs and CTD data shown in Figure 5.2 it is evident that while both UOI and MvOI brought the temperature field closer to the observed, only the MvOI improved the salinity as well. However, the improvements are not as marked as for the UOI with salinity adjustments presented earlier. Different ratios of observational to forecast error variance were used in those experiments so the results require closer scrutiny.

The error covariance matrix of the MvOI was expressed in terms of empirical orthogonal functions (eofs) which offer a way to compactly store the matrix and isolate the leading directions of variability and possibly further reduce the dimension of the problem. How well does a particular set of eofs estimated from an ensemble of snapshots represent the dominant error subspace? Does this subspace vary significantly with season or exhibit interannual variability? To answer these questions we projected an ensemble of ocean state anomalies at an arbitrary date onto a given set of eofs and analyzed the residuals. If the residuals from the projection (i.e. that portion of the "signal" that is not in the space spanned by the eofs) are noise-like, this means that the eofs captured the significant information regarding the model error covariance structure.

We examined the residuals using several sets of basis eofs and several sets of states projected onto these bases. Our analysis indicated that the model error covariance matrix could be represented by a reduced set of eofs, allowing for an efficient analysis and that the covariance estimates appear to be robust in that the model error covariance structure does not exhibit significant seasonal or interannual variations.

We are now in the process of implementing this methodology for the global model. In doing this, we are exploring ways to most efficiently and effectively generate the ensembles and keep the ensemble size small. We are also exploring ways to include sources of error beyond those due to surface forcing.

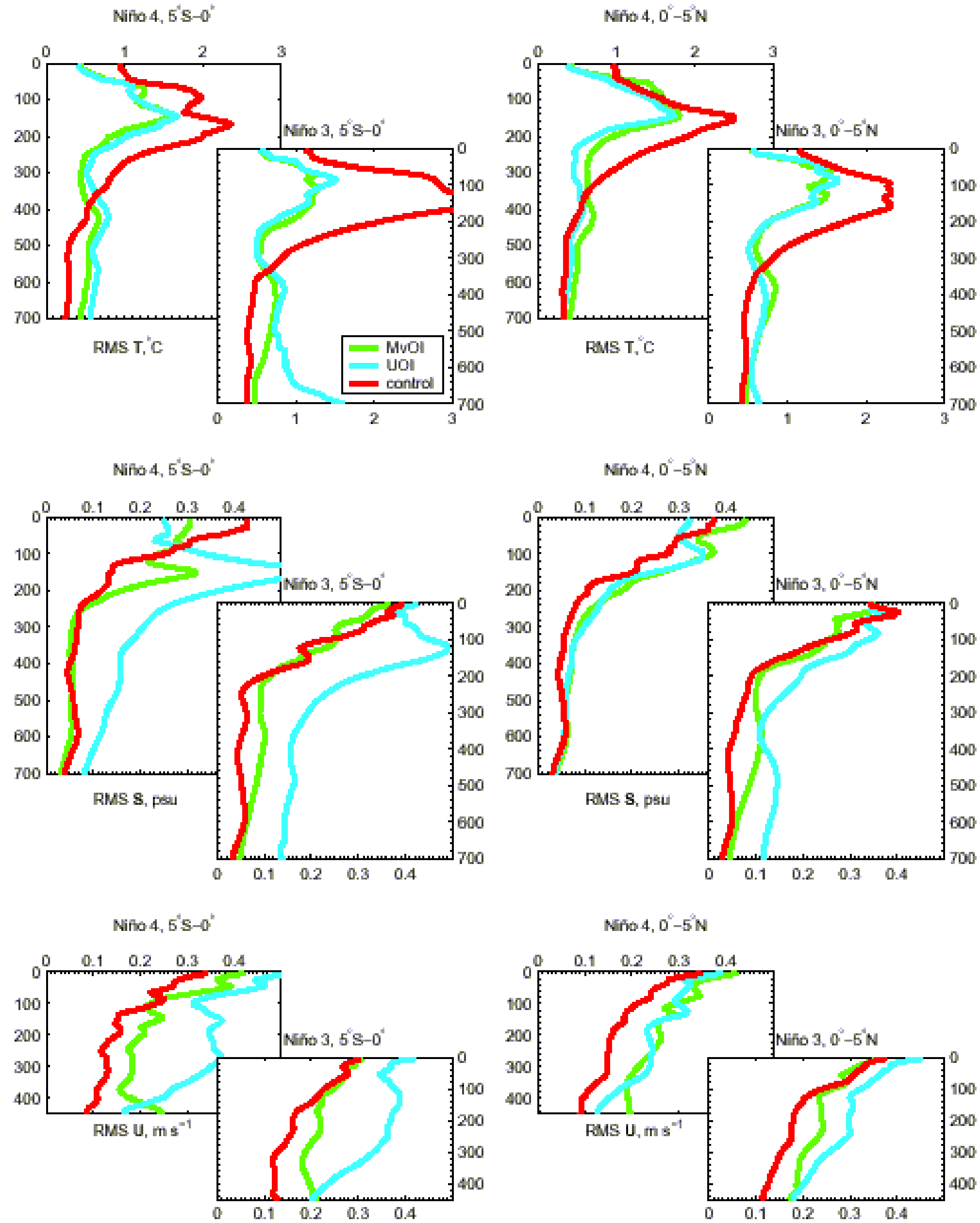

Figure 5.2 RMS difference between simulations and data for temperature and salinity, averaged over all available CTD profiles for the period 7/1996 - 12/1998 (Johnson et al., 2000). Temperature (a,b,g,h), salinity (c,d,i,j) and zonal velocity (e,f,k,l) data is shown for northern and southern halves of the Niño 3 (150ºW-90ºW) and Niño 4 (160ºE-150ºW) regions.}

5.4 Multivariate Ensemble Kalman Filter Development and Applications

Accounting for biased model errors

As with most ocean models, the vertical structure from the Poseidon model in the equatorial region suffers from systematic biases. This is especially true for temperature as the thermocline layer becomes too diffuse in response to vertical diffusion. At present, the three components of the NSIPP ODAS do not explicitly account for the model bias. Rather, like most data assimilation methods, these algorithms are derived under the assumption that the data errors as well as the models errors have unbiased statistical distributions. In practice, this seems to have repercussions only during the first few analyses during which the initial effect of the temperature assimilation is to tighten the thermocline along the Equator. Once this adjustment has taken place, the assumption of unbiased forecast errors is approximately satisfied and further improvements caused by the assimilation are mainly the result of correcting the unbiased error component.

Although the assumption of unbiased model errors appears to have only a small repercussion over the long run, we have adapted a recent algorithm (Dee and DaSilva 1998), which is theoretically valid even with biased prognostic fields, to the NSIPP ODAS framework. Initial tests with the new bias-correction algorithm with the MvEnKF indicate that the time-mean model fields converge to the time-mean observations faster than when the bias-correction algorithm is not used. Figure 5.3 illustrates the application of the bias estimation algorithm with the MvEnKF in a 60-day TAO-temperature assimilation experiment starting on January 1, 1996 by showing the evolution of the estimated temperature bias along the Equator. The left panels correspond to the temperature increments. The right panels show the bias estimate. In the absence of a priori information about the model drift, the initial bias estimate before the first analysis is zero everywhere. In the first analysis (top panels), the temperature-field correction is large (left) and the bias estimate is small (right). After about 20 days, the temperature field corrections have become much smaller than the initial correction as the model estimate has improved in response to the earlier analyses. Between 20 days and 60 days, the bias estimate continues to evolve (bottom three right panels) as more information about the model error distribution becomes available, although the changes are not as important as during the first 20 days of the experiment. We are currently in the process of fine-tuning the bias-correction scheme in the light of this encouraging initial result and have undertaken experiments to assess the impact of the bias correction on the quality of the assimilation products.

Temperature data assimilation

Since the last progress report, we have submitted two articles discussing the application of the MvEnKF to the assimilation into Poseidon of TAO temperature data (Keppenne and Rienecker, 2002a, 2002b). As well as documenting our assimilation system, we have undertaken a cross-validation of the multivariate assimilation of temperature data by examining how the corrections applied to the *T, S,* u and *v* fields when the TAO-temperature data are processed affect the accuracy of the model velocity and surface height fields. Independent acoustic Doppler current profiler (ADCP) current data and T/P SSH anomalies were used for this purpose.

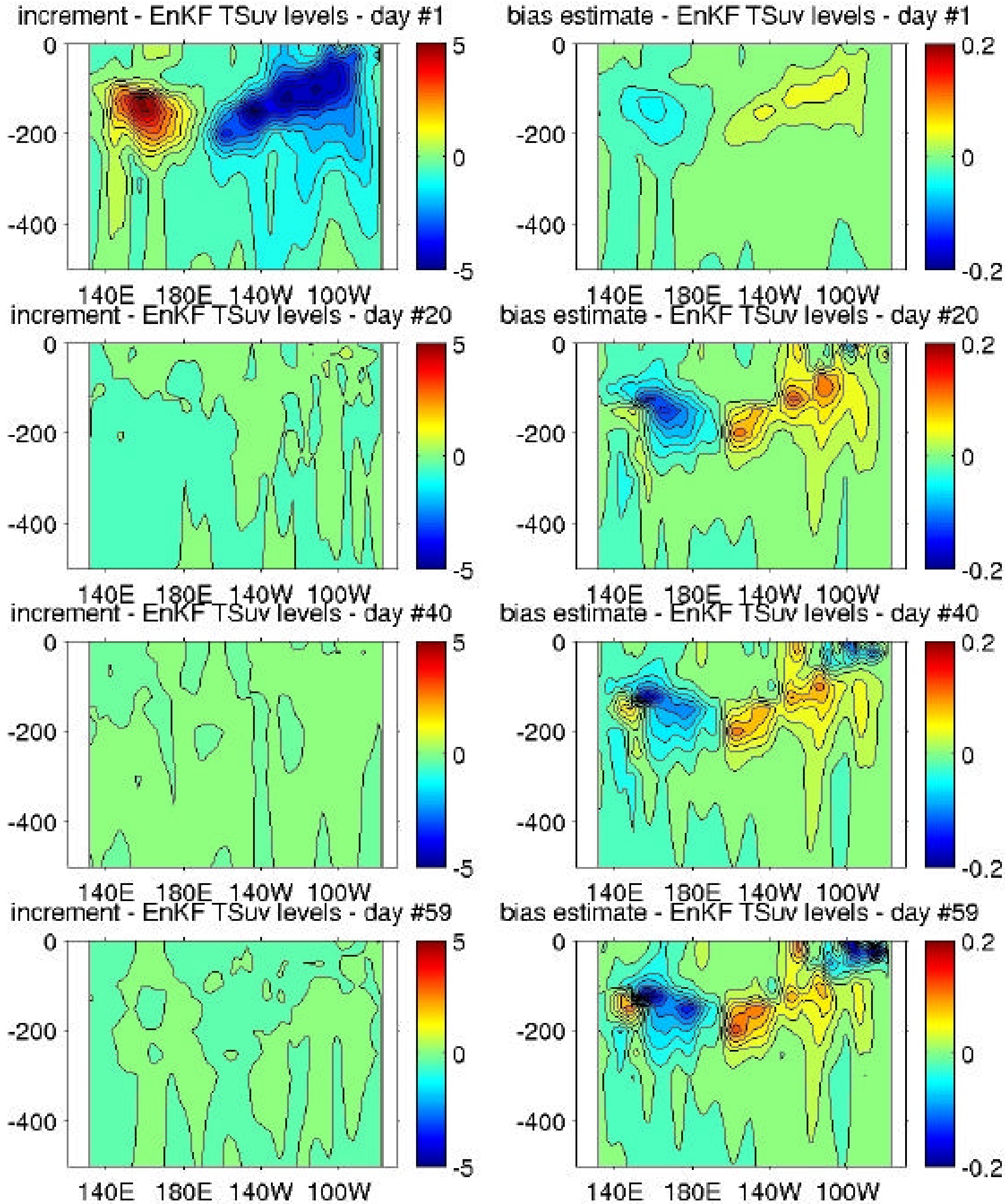

Figure 5.3 Evolution of the temperature increments along the Equator (left) and of the temperature-bias estimate (right) in a 60-day TAO-temperature assimilation experiment with the MvEnKF. From top to bottom: initial increment and bias estimate after the first analysis (top) followed by increments and bias estimates at 20 days (second row), 40 days (third row) and 60 days (bottom).

One of the important issues with the MvEnKF is the validity of its forecast error estimates. With the MvEnKF, the error variance (main diagonal of $\boldsymbol{P}^f$) is estimated by measuring the ensemble spread. Figure 5.4 shows how the ratio of the root-means-square (RMS) ensemble spread for temperature (EnRMS) to the RMS temperature innovation (RMSI) evolves during a three-month period during which TAO temperature data are assimilated into Poseidon every five days. The EnRMS is calculated before each analysis, after interpolation of the model temperature field to the location of each TAO measurement. It estimates the RMS forecast error for temperature. Its ratio to the RMSI is thus an indicator of how well the ensemble spread accurately predicts the RMS error.

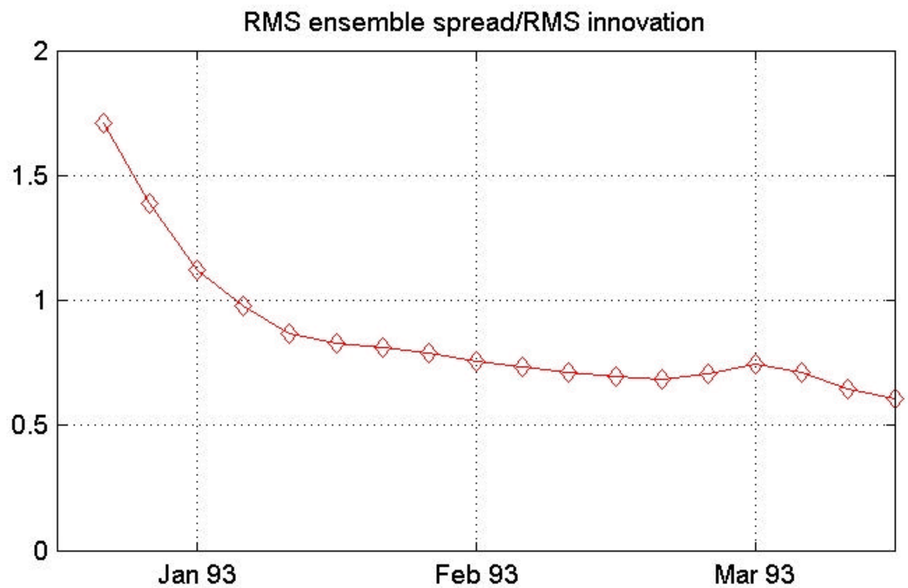

Figure 5.4 Evolution of the ratio of the RMS ensemble spread for temperature (taken at the location of each measurement) to the RMS temperature innovation during a three-month TAO-temperature assimilation experiment. The diamonds indicate the time of each analysis.

The ratio of the EnRMS to the RMSI drops to a value of 0.98 between the first and fourth analyses. Hence, the ensemble spread is in good agreement with the actual errors at the time of the fourth assimilation. After the fifth analysis the RMS ratio keeps declining, albeit more slowly than between the first and fifth analyses. Moreover, the rate at which the RMS ratio declines between two successive analyses is roughly constant after the fifth analysis. A plausible explanation is that the process-noise model does not account for enough variability since, at present, the system noise is represented solely by modeling the errors in the surface wind stress and heat flux forcing. In order for the RMS ratio to stay close to unity until the end of the experiment, it will be necessary to include a term to simulate the model errors in the system noise representation. Such a system noise representation is in development. Without it, the data assimilation would eventually fail if the experiment were continued for several years. The failure would result from the MvEnKF gradually attributing less weight to the observations even though the forecast does not become gradually more accurate after the RMSI has reached a steady state.

Ongoing developments

Following the promising results encountered in using the MvEnKF to process observations with the Pacific basin version of Poseidon, our highest priority now is to apply the algorithms to assimilate data into the global version of the OGCM--in preparation for integrating the MvEnKF into the NSIPP coupled forecasting system.

6. Land Data Assimilation

Seasonal climate forecasting must rely on the correct initialization of the slow components of the Earth system, namely the oceans and the land surface. At the land surface, soil moisture controls the partitioning of moisture and energy fluxes to the atmosphere and is a key variable in weather and climate prediction. The memory associated with soil moisture is likely the chief source of forecast skill for mid-latitude continental summer precipitation (Koster et al., 2000).

The main focus of the NSIPP land assimilation effort has been to assess the relative merits of the Ensemble Kalman filter (EnKF) and the Extended Kalman filter (EKF) for soil moisture initialization within the NSIPP forecast system. Both assimilation algorithms take into account model as well as measurement uncertainties and provide dynamically consistent estimates of the soil moisture state. In a fraternal twin experiment for the south-eastern United States we assimilated synthetic observations of near-surface soil moisture once every three days, neglecting horizontal error correlations and treating catchments independently (Reichle et al., 2001). We calibrated the model error variances for both filters such that they perform as best as they can, using as an aggregate performance measure the sum of the average actual errors in the surface excess, the root zone excess, and the catchment deficit (Figure 6.1). After calibration, both filters provide satisfactory estimates of soil moisture (Figure 6.2). The average actual estimation error in the (volumetric) moisture content of the soil profile is 1.64 % for the EKF, 1.62 % (or 1.49 %; or 1.40 %) for the EnKF with 4 (or 10; or 500) ensemble members, and 5.59 % without assimilation. This implies that in our application, the EKF and the EnKF with four ensemble members are equally accurate at comparable computational cost. We also demonstrated that nonlinearities in soil processes are treated adequately. While expected error covariances of both filters are largely in agreement, they generally differ from actual estimation errors. This is attributed to the less than perfect representation of the model errors in our synthetic experiment.

Perhaps the most difficult part of implementing any data assimilation method is to determine appropriate model error covariances. This problem is confounded by the scarcity of independent data that would allow us to verify the soil moisture estimates from the assimilation system on a global scale. In our synthetic experiment, we simply used the actual errors (estimate minus synthetic truth) as an objective criterion to select appropriate model error variances, but this is of course impossible when satellite data are assimilated. Fortunately, all data assimilation systems produce innovations (observations minus model forecast). Most recently, we have demonstrated that the innovations that are produced by our EnKF land assimilation system contain valuable information about the validity of the assumed model error covariances (Reichle and Koster, 2002). It turns out that the statistics of the innovations can be used as an indicator of estimation accuracy and thereby for identifying appropriate model error covariances.

In summary, the key advantages of the EnKF for land assimilation are:

(1) The EnKF performance can be increased by increasing the ensemble size.
(2) The EnKF can account for a wider range of model errors.
(3) The EnKF can be extended to account for horizontal error correlations.

If present, horizontal correlations allow spreading information to unobserved locations. Because of its flexibility and its performance in our study, the EnKF is the more promising approach for soil moisture initialization problems.

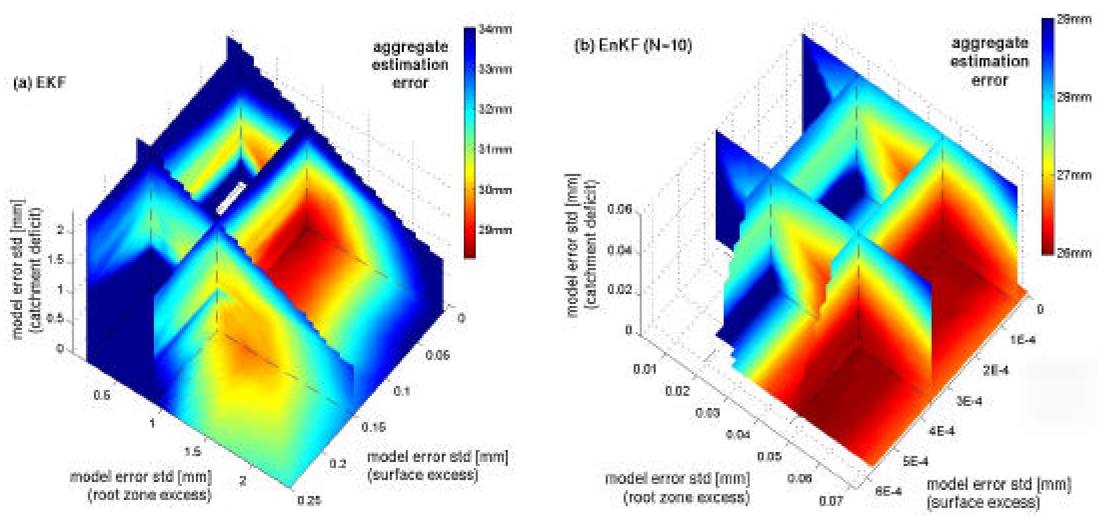

Figure 6.1 Aggregate estimation error as a function of the model error standard deviations for the (a) EKF and (b) EnKF with N=10 ensemble members. The difference in scales in the aggregate estimation error reflects the superior performance of the EnKF. The difference in scales in the model error parameters is due to the difference in model error correlation times (EKF requires white model errors while in the EnKF we use a three-day correlation time).

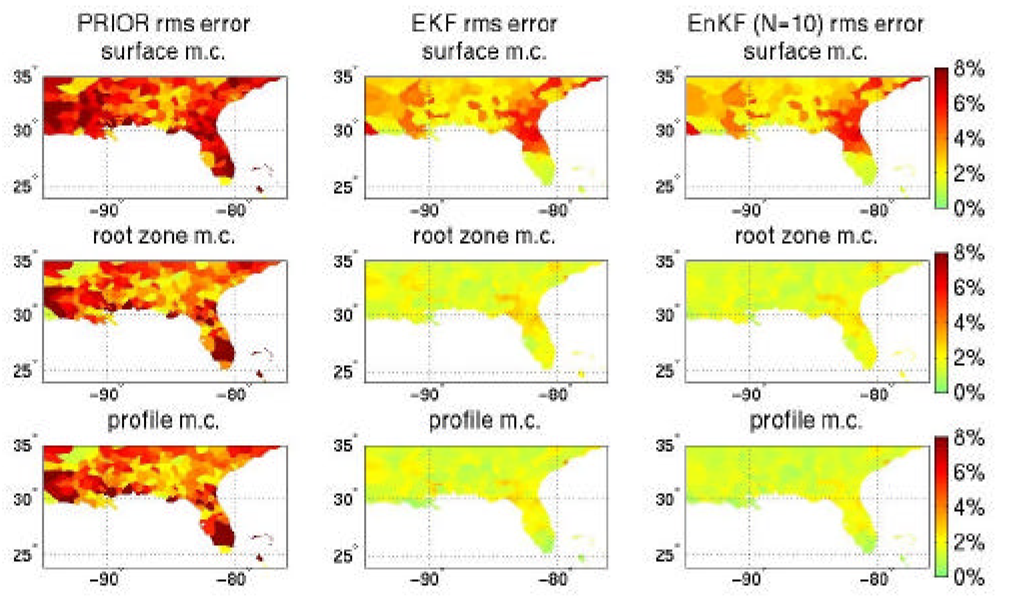

Figure 6.2 Time-average error of the moisture content (m.c.) prior to assimilation, for the EKF, and for the EnKF with N=10 ensemble members. Units are volumetric moisture percent.

7. Atmospheric Model Development

7.1 Atmosphere

Major modifications were undertaken in the physical parameterizations used by the NSIPP atmospheric general circulation model (AGCM). These modifications were aimed primarily at improving the model's simulation of boundary layer clouds over the ocean, especially maritime stratus decks and the stratus - trade cumulus transition. A prognostic cloud condensate scheme was implemented, as well as a shallow convection/PBL entrainment parameterization scheme. Changes to existing parameterization schemes, including convection, radiation and turbulence schemes were also made.

The prognostic cloud scheme implemented in the NSIPP AGCM borrows from the earlier schemes of Del Genio et al. (1996) and Sud and Walker (1999). Two sources of cloud condensate are included - from detraining convection, and from large-scale (or statistical) condensation. The statistical source is parameterized by assuming a uniform PDF of specific humidity, with a width given by a fraction of the local saturated value. Cloud fraction (by volume) is kept as a prognostic variable as well as cloud condensate mixing ratios as in Tiedtke (1993). This is especially useful in determining cloud fraction produced by convective mass fluxes.

Losses of cloud condensate, l, and cloud fraction occur through of a variety of microphysical processes. These processes include autoconversion of cloud water to precipitation (A), collection or accretion of cloud water by precipitation (C), and evaporation (E) (Figure 7.1). Autoconversion from cloud condensate to precipitation is formulated as in Sundqvist (1989) and Sud and Walker (1999). Evaporation of cloud condensate is formulated according to Del Genio et al. (1996). A final pathway in the AGCM water cycle is given by re-evaporation of precipitation R, which is formulated analogously to condensate evaporation.

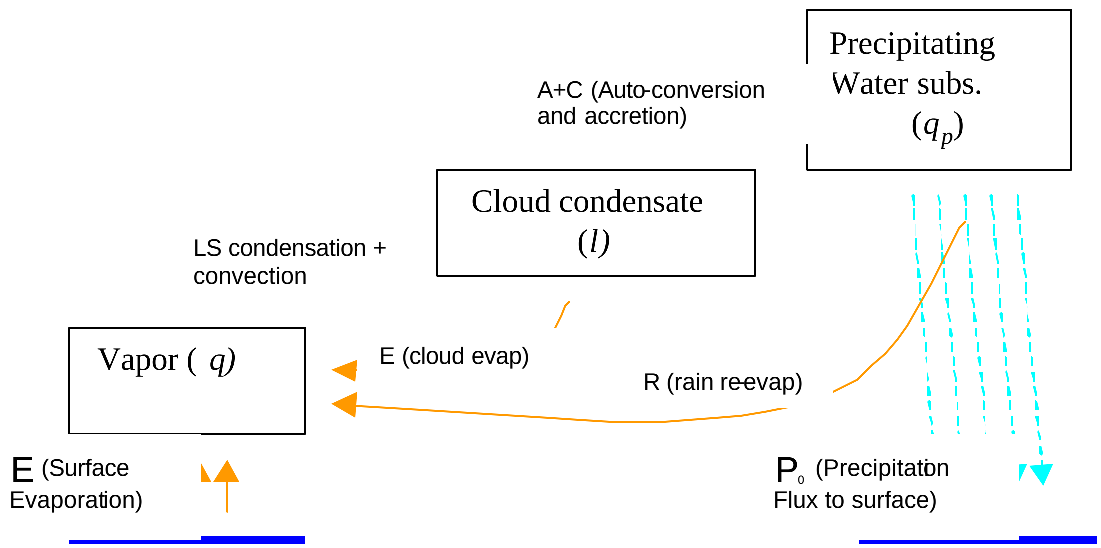

Figure 7.1 Schematic of water cycle in AGCM with prognostic

Unfortunately, little observational guidance exists for the relative global magnitudes of these conversion terms (except for E and P_0). Satellite estimates for the reservoirs q and l exist and can provide some information. Examples of vertically integrated conversion terms as well as q and l from a recent short (5-month) AGCM experiment are shown below in Figure 7.2. The sizes of the vertically-averaged reservoirs q and l averaged between 40S and 40N are in rough agreement with satellite estimates (not shown). The sizes of the loss terms for liquid water are comparable to those reported in Rostayn (1999). It is important to note that the relative importance of the conversion terms is sensitive to the choice of tunable parameters. It is possible to obtain equally reasonable simulations of q and l with different parameter choices. Careful tuning of these parameters has yet to be performed.

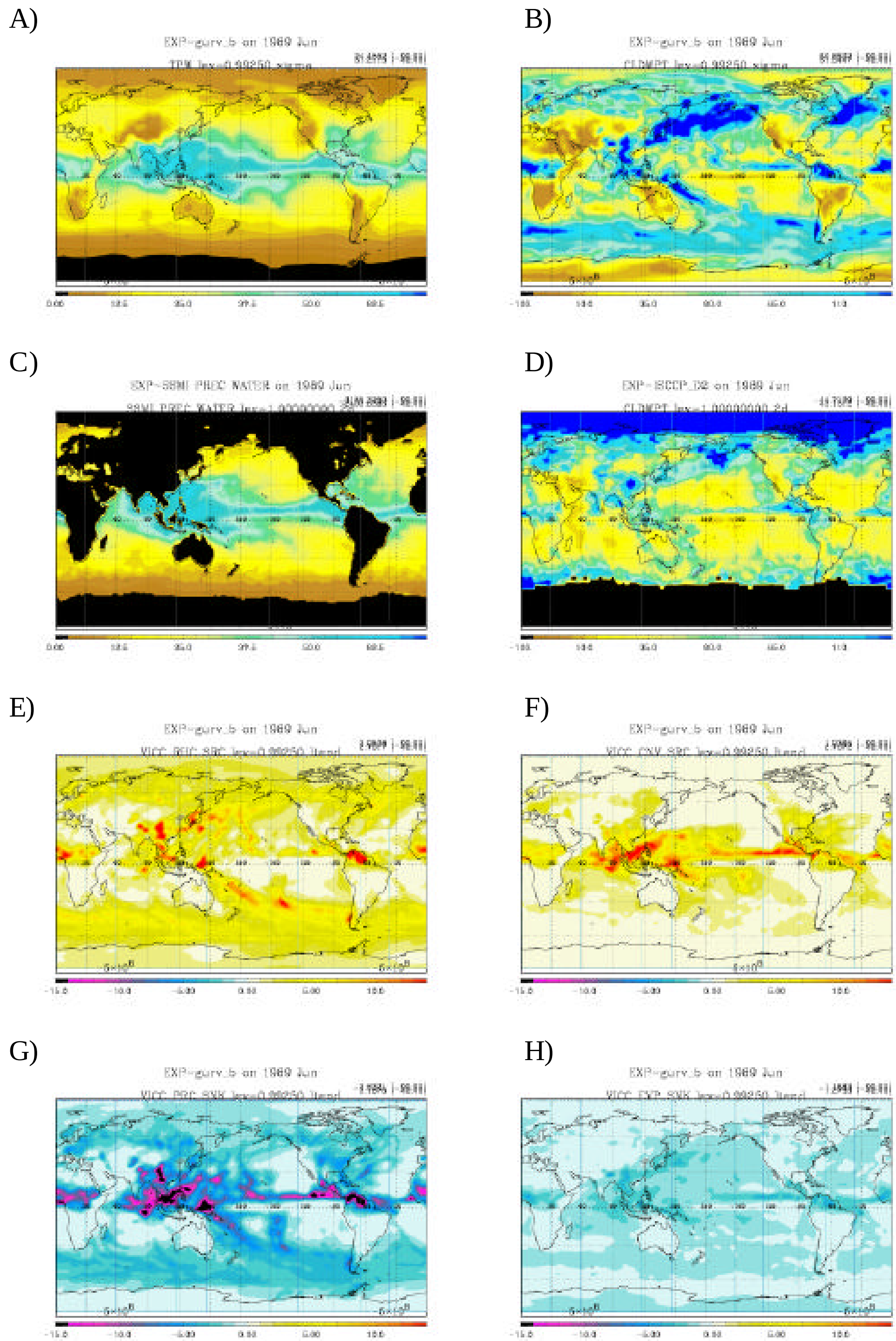

Figure 7.2 (a) Total precipitable water from NSIPP AGCM for June 1989 as a function of latitude and longitude in kg m^{-2}; (b) liquid water path in g m^{-2} ; (c) SSMI estimate of total precipitable water (kg m^{-2}); (d) ISCCP estimate of cloud liquid water path (g m^{-2}) ;(e) vertically integrated source of condensate from large scale condensation in kg m^{-2} d^{-1} ; (f) vertically integrated source of condensate from convection in kg m^{-2} d^{-1}; (g) vertically integrated loss of condensate from due to autoconversion in kg m^{-2} d^{-1} ; (h) vertically integrated loss of condensate from due to evaporation in kg m^{-2} d^{-1}.

Entrainment/Shallow Convection

Adequate simulations of maritime stratus decks in AGCMs are as likely to depend on boundary layer parameterizations as on inclusion of detailed cloud microphysics. Numerous investigators have suggested that the key to simulating realistic boundary layer clouds lies in correctly diagnosing the rate of entrainment at the top of the boundary layer (e.g., Grenier and Bretherton, 2001). Moisture and potential temperature gradients at the top of the stratus-capped maritime boundary layer are strong, so that small differences in turbulent transport can have a large impact on cloud distributions. Standard dry turbulence schemes tend to underestimate PBL-top entrainment, leading to overly wet, cool marine BLs and excessive low cloud cover.

The NSIPP AGCM includes a simple 1st-order, dry PBL scheme (Louis et al., 1983). The scheme appears to perform well in many respects, such as in its overall reproduction of tropical temperature and moisture profiles. However, without modification, the scheme leads to excessive low-level cloudiness throughout the sub-tropics. In order to overcome this problem, a relatively simple, plume-based entrainment calculation was added to the basic Louis scheme. This calculation is accomplished using a 1D linearly entraining moist plume model to estimate the strength of overshooting moist thermals originating from the surface layer, (Figure 7.3).

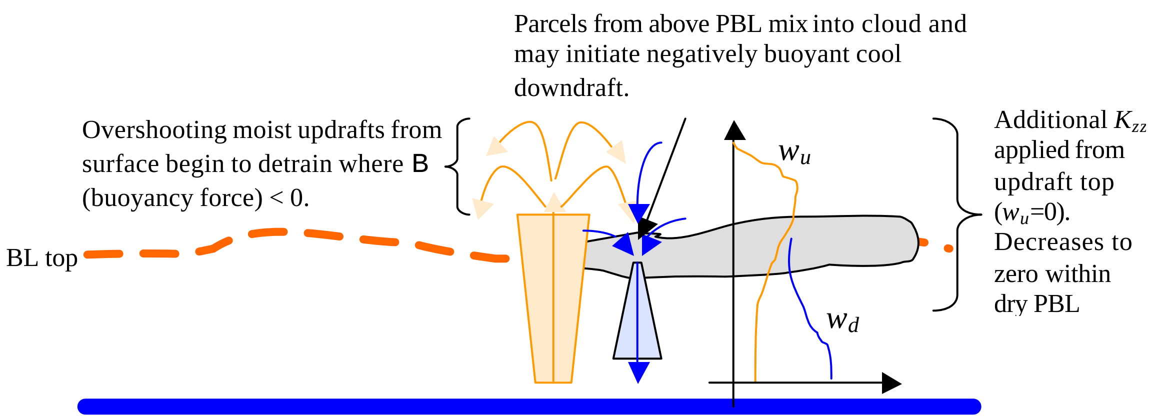

Figure 7.3 Schematic diagram of plume based PBL-top entrainment parameterization. Moist plumes from surface layer penetrate top of BL due to added buoyancy from moist condensation. Parcels from free atmosphere are forced into cloudy PBL by detraining moist updrafts. Evaporative cooling can destabilize parcel with respect to surroundings.

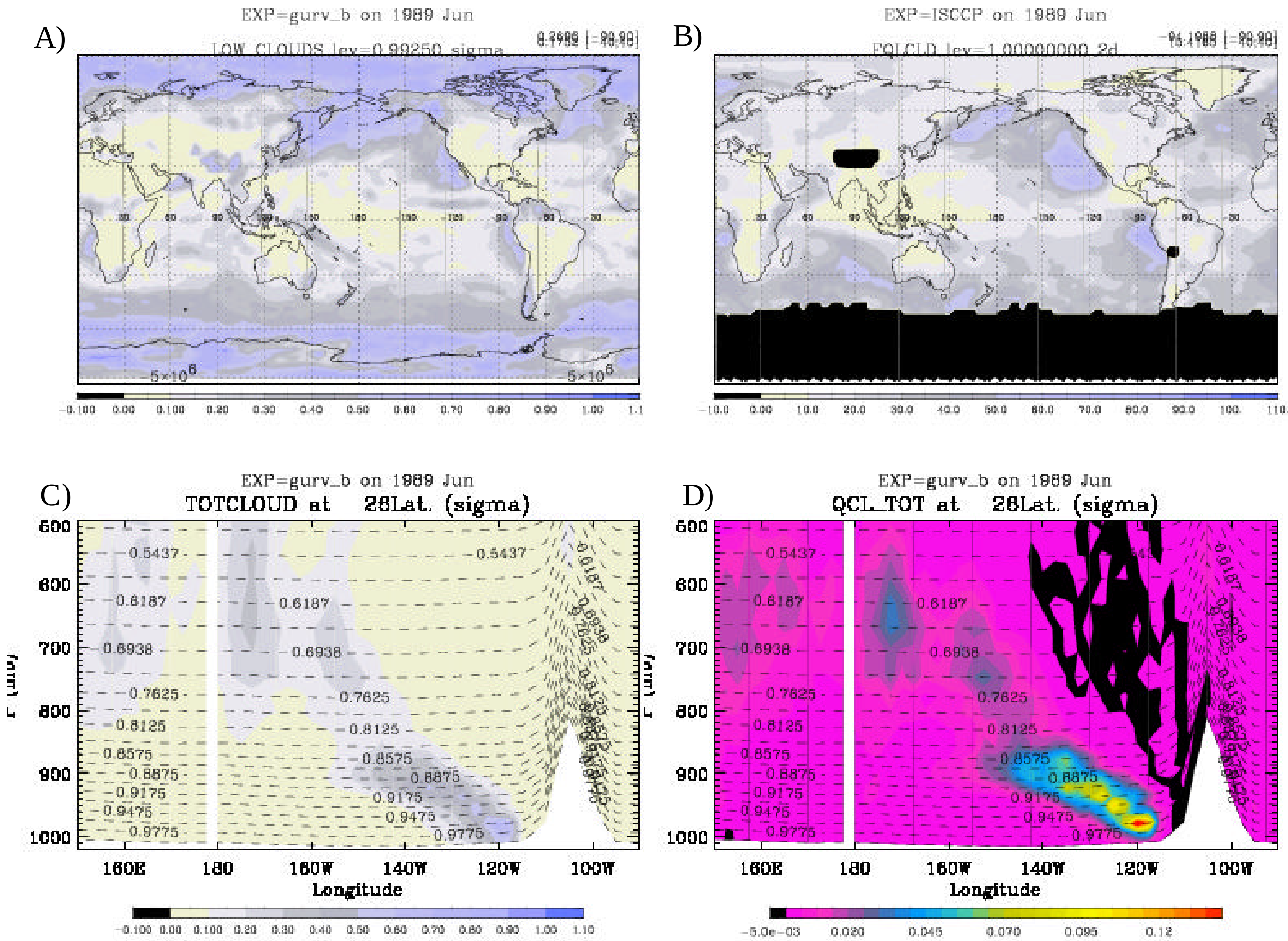

Figure 7.4 (a) low level (>700mb) cloud cover for June 1989 from the NSIPP AGCM with prognostic clouds and PBL entrainment; (b) ISCCP low cloud fraction for June 1989; (c) longitude-pressure section along 26N – California stratus region – of cloud fraction from the model; and (d) longitude-pressure section along 26N of cloud condensate mixing ratio (g/kg).

This parameterization is intended to simulate the effects of shallow moist convection and cloud top entrainment instability on boundary layer structure, and, in particular, to capture the break-up of marine stratus decks over subtropical oceans. Tests with the NSIPP AGCM show some success in these areas. Figure 7.4 shows maps of low cloud cover as well longitude-pressure sections through the California stratus region (~26N) from the same model experiment used to produce Figure 7.2. Comparison with ISCCP data (Figure 7.4b) shows general agreement in pattern. The model's stratus decks are not extensive enough, while midlatitude-polar cloudiness is too high. The cross-sections (Figures 7.4c, d) reveal what appears to be a qualitatively reasonable distribution of clouds and cloud condensate in the California stratus region. The simulated cloud decks slope gradually upward in the west, reaching heights of around 1000m near 150W, before breaking up into shallow cumulus. Peak condensate mixing ratios are somewhat low. It is not yet clear whether this is related to microphysical or turbulent processes.

Double ITCZ sensitivity studies

Along with the introduction of new physical parameterizations in the NSIPP AGCM, extensive parameter sweeps were done with the previous “frozen” version of the model (patch4, NSIPP1). The aim of these studies was to identify factors controlling the formation of so-called double ITCZs in the model tropics.

For most of the year, observed rainfall shows a single ITCZ in both the Pacific and Atlantic that is located 5-10 degrees north of the Equator. AGCMs frequently show a pronounced second ITCZ, especially in the Pacific, at similar latitudes south of the Equator. Anecdotal evidence suggests that the appearance or disappearance of double ITCZs in AGCM simulations may be sensitive to a number of convection related parameters. The particular sensitivity appears to be highly model dependent and the sensitivity found in one model does not necessarily carry over to other models. In the NSIPP AGCM the double ITCZ responds to changes in microphysical parameters used within the convection parameterization.

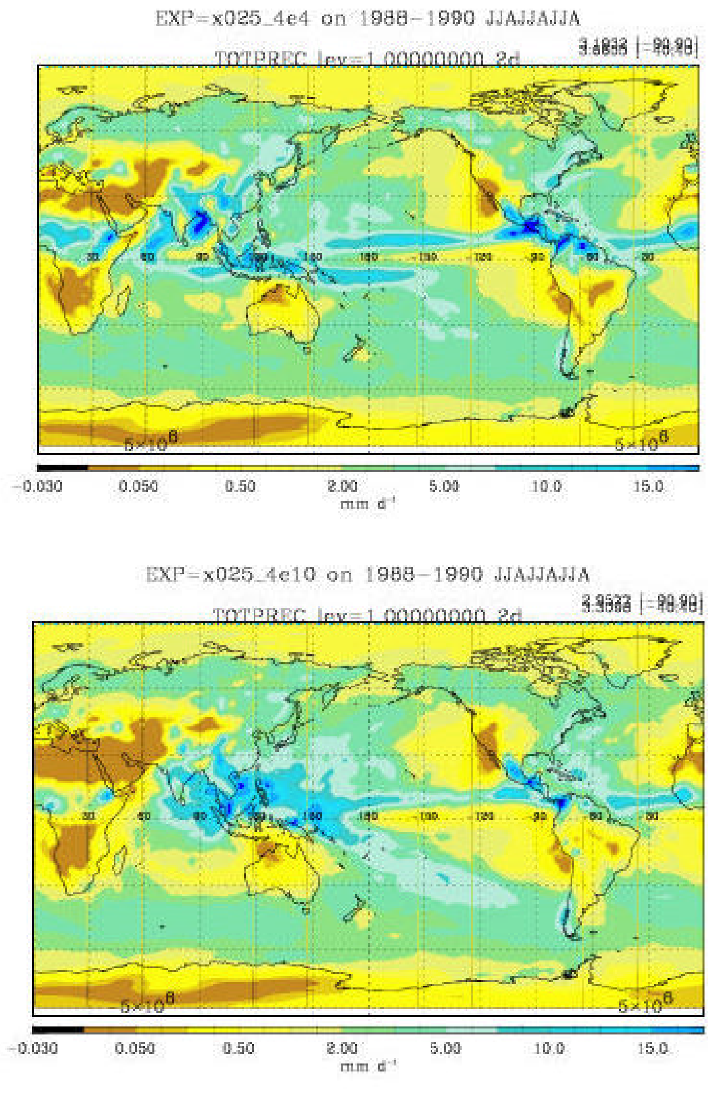

Figure 7.5 Three season mean precipitation June-August 1988-1990 from two AGCM experiments. Top panel has rapid autoconversion and weak rain re-evaporation. Bottom panel has slow autoconversion and strong rain re-evaporation.

Figure 7.5 shows precipitation from two experiments with different microphysical rate constants employed within RAS. One experiment (Figure 7.5, top) has efficient convective precipitation, i.e., rapid autoconversion and weak rain re-evaporation, the second (Figure 7.5, bottom) has inefficient convective precipitation. The case with high efficiency exhibits a pronounced double ITCZ, while in the case with low efficiency a single ITCZ is present. These experiments used an earlier version of the NSIPP AGCM with diagnostic clouds and no PBL entrainment, but recent experiments with the latest version of the model exhibit a similar sensitivity.

7.2 Land Surface Model Development

As reported last year, Sarith Mahanama, a post-doctoral associate, tested the NSIPP-Catchment model offline in the Torne/Kaliz River system in northern Scandinavia as part of the PILPS 2E project. This year saw the completion of those tests and the further testing of the model across a large section of the Rhone River basin as part of the GSWP Rhone-AGG model intercomparison experiment. The catchment model performed quite well in both tests.

Model development this past year has focused on improving runoff generation through improved treatments of "stormflow" and baseflow, through collaborative work with Marc Stieglitz of Columbia University. Stormflow is subsurface lateral flow above the main water table (e.g., due to perched water tables) that responds more slowly to precipitation than surface runoff but much more quickly than baseflow. Stieglitz's group has developed a simple approach for modeling stormflow (Shaman et al., submitted), and a version of their scheme has been successfully tested in the NSIPP-Catchment model. Baseflow generation in the real world is affected by spatial variability in bedrock depth, which results, for example, from the accumulation of soil in lowland areas at the expense of hilltops. Working with Stieglitz's group, we have successfully tested an approach for including this effect in the NSIPP-Catchment model. Stieglitz's group was also instrumental in the complete recoding of the snow module into a more reliable form that is also more suitable for snow data assimilation studies.

Global datasets of model parameters have been improved. Colin Stark of Columbia University has provided NSIPP with a rasterized description of catchment locations across the globe, a dataset much more amenable to manipulation than the polygon description used earlier. Using Stark's dataset, Sarith Mahanama has processed the catchment topography, soil, and vegetation information into global datasets of NSIPP-Catchment model parameters, setting the stage for AGCM simulations with the NSIPP-Catchment model. Preliminary simulations have indeed been performed with the coupled models. Relative to the Mosaic model (which is used operationally in the NSIPP system), the NSIPP-Catchment model seems to produce less precipitation over land in many regions, bringing the simulated precipitation more in line with observations (Figure 7.6). More work needs to be done in the coming year, however, to evaluate the NSIPP-Catchment model's behavior in the coupled system.

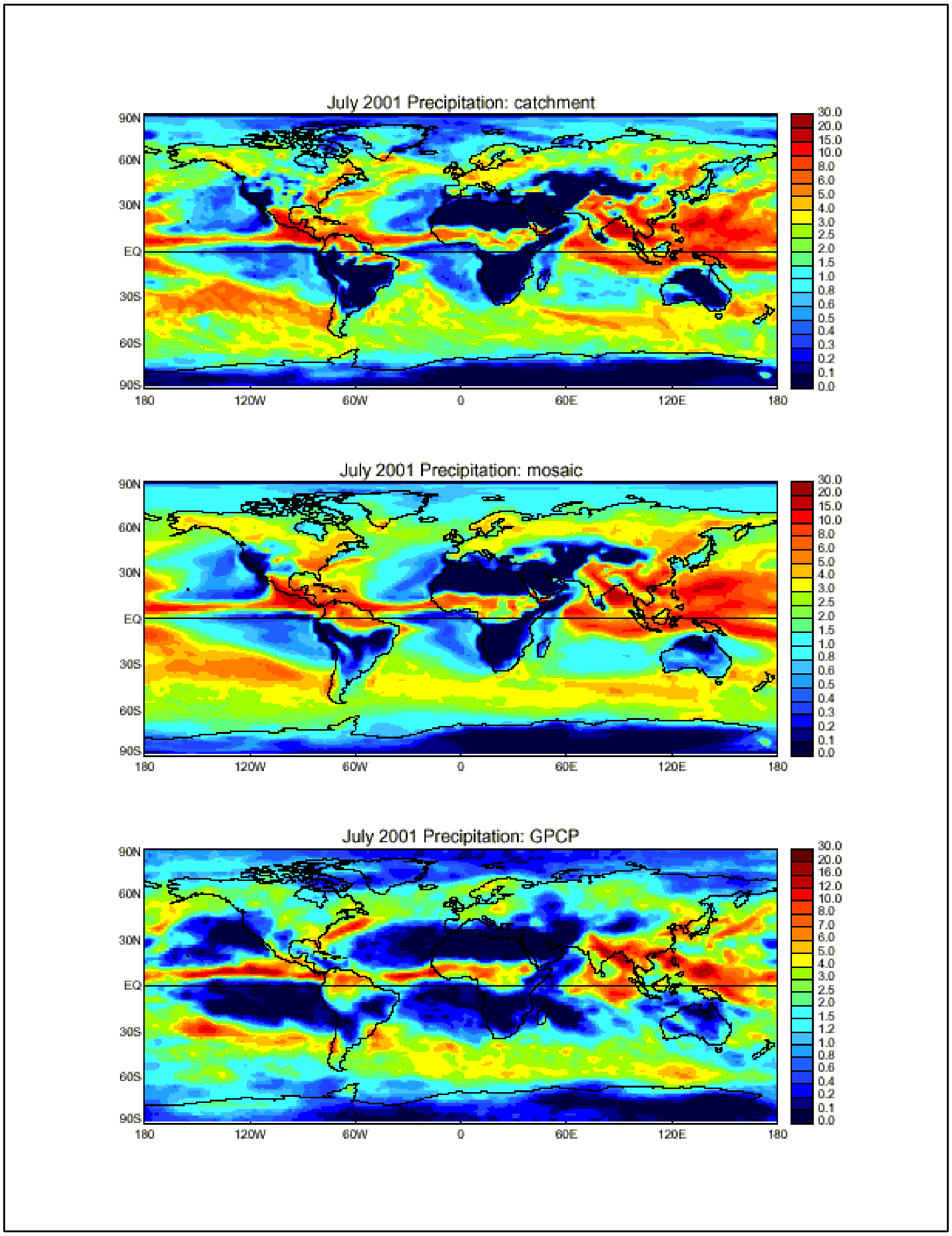

Figure 7.6 First look at the impact of the new land surface scheme on precipitation in the NSIPP system. Top: July 2001 precipitation generated by the NSIPP AGCM coupled to the NSIPP-Catchment model (single realization), following several years of spin-up. Middle: July 2001 precipitation generated by the NSIPP AGCM coupled to the Mosaic land surface model (average of 16 realizations), following several years of spin-up. Bottom: Observed July 2001 precipitation from GPCP. Units are mm/day.

8. Other Investigations

8.1 Equatorial Pacific Waves on Seasonal and Interannual Timescales

An ocean hindcast for the period of 1988-98 was used to study equatorial wave processes and their role in interannual variations along the equator. It was found that the reflection of the interannual Rossby waves at the Pacific western boundary is far from the linear theory, suggesting strong nonlinearity in the western boundary reflection. In contrast, the reflection of the Kelvin waves at the Pacific eastern boundary is in perfect agreement with the linear theory. The western boundary reflection is found to play a very important role in ENSO.

The roles of the Kelvin and Rossby waves in the seasonal cycle of the equatorial Pacific were also investigated. The reflection of the first baroclinic Kelvin and Rossby long waves at the western and eastern boundaries is in good agreement with linear theory. The semi-annual signals in the far eastern equatorial Pacific were strongly influenced by the semi-annual oscillations in the far western Pacific. In contrast, the semi-annual oscillations in the far western Pacific were influenced very little by the semi-annual signals in the far eastern Pacific. Instead, they were forced by the local monsoon and the Rossby waves from the central-eastern equatorial Pacific.

8.2 Atmospheric Circulation and Precipitation Over South America

South American circulation and precipitation are modulated by the Southern Oscillation (SO) in interannual timescales and by the South Atlantic Convergence Zone (SACZ) and frontal passages on submonthly timescales. Observed and reanalysis datasets, as well as NSIPP1 simulations are being used to study how the SO and SACZ affect the South American low-level jet (SALLJ), the Amazon and Atlantic Intertropical Convergence Zones (ITCZs), the water budget over South America, and the precipitation and convective system formation over South America.

SO-Related South American Circulation and Precipitation Variability and Predictability

NSIPP1 AMIP-style simulations reproduce the mean observed JFM circulation over South America during normal years. During Niño years the AMIP simulations capture the observed enhanced trade winds and decreased precipitation in the Amazon Basin and Atlantic ITCZ, as well as the observed enhancement of the SALLJ and some of the observed enhancement of precipitation in subtropical South America.

A 20-year long NSIPP1 'perpetual Niño' simulation was produced by forcing the model with SSTs that consisted of climatological SSTs plus Pacific Niño SST anomalies. The results obtained in the 'perpetual Niño' simulation were very similar to those of the Niño years in the AMIP simulation, suggesting that Pacific Ocean SST anomalies alone determine most of the observed strengthening of the South American Monsoon System observed during Niño years. This includes the strengthening of the SALLJ, the increase in trade easterlies and decrease in precipitation in the Atlantic ITCZ and Amazon Basin, and, to a lesser extent, the increase in precipitation over subtropical South America.

Preliminary analysis of the NSIPP1 Dynamical Seasonal Prediction simulations suggests that there is hope for predictability of the summertime precipitation and circulation in South America.

The interannual variability of the tropical precipitation and circulation in South America and adjoining oceans is dominated by signal, that is, by the interannual variability of SST anomalies. The SALLJ and SACZ are less predictable because they are strongly influenced by baroclinic waves whose nature is much more chaotic.

Variability of South American Convective Cloud Systems and Circulation During January-March 1998 and 1999

According to the NCEP reanalysis, the South American low-level jet (SALLJ) was nearly twice as strong during January-March (JFM) of the 1998 El Niño episode than during JFM of the 1999 La Niña episode. The difference in SALLJ strength between these two years translated into a stronger transport of moist tropical air into the subtropics during JFM98 than during JFM99. An objective analysis technique was used to identify large, long-lived convective cloud systems in infrared imagery. The stronger SALLJ resulted in larger and more numerous convective cloud systems and nearly twice as much rainfall in subtropical South America (parts of Southern Brazil, Uruguay, and Argentina) during JFM98 than during JFM99. The difference between JFM98 and JFM99 SALLJ strength in Bolivia is explained in part by submonthly variability associated with the SACZ, but also by interannual variability associated with the Southern Oscillation.

In the tropical portions of South America nearly six times more convective cloud systems were observed during JFM99 than during JFM98. This was accompanied by more plentiful precipitation in the Amazon basin and in the Bolivian Altiplano during JFM99 than during JFM98. Interannual variability associated with the Southern Oscillation was an important contributor to the observed convective cloud system and precipitation differences in tropical South America.

References

Deardorff, J. W., 1980: Cloud-top entrainment instability. *J. Atmos. Sci.*, 37, 131–147.

Dee D. P., and A.M. da Silva, 1988: Data assimilation in the presence of forecast bias. *Quart. J. Roy. Meteor. Soc.*, 124, 269-295.

Del Genio, A. D., N.-S. Yao, W. Kovari, and K. K.-W. Lo, 1996: A prognostic cloud water parameterization for general circulation models. *J. Climate*, 9, 270–304.

Grenier, H. and C. S. Bretherton, 2001: A moist PBL parameterization for large-scale models and its application to subtropical cloud-topped marine boundary layers. *Mon. Wea. Rev.*, 129, 357-377.

Hess, P.G., D.S. Battisti and P. Rasch, 1993: Maintenance of the Intertropical Convergence Zones and the Large-Scale Tropical Circulation on a Water Covered Earth. J. Atmos. Sci., 50, 691-713.

Ji M., A. Leetmaa and J. Derber, 1995: An Ocean Analysis System for Seasonal to Interannual Climate Studies. *Mon. Wea. Rev*., 123, 460-481.

Johnson, G.C., M. J. McPhaden, G. D. Rowe, and K. E. McTaggart, 2000: Upper equatorial Pacific ocean current and salinity variability during the 1996-1998 El Niño-La Niña cycle, *J. Geophys. Res.*, 105, 1037-1053.

Keppenne, C., and M. Rienecker, 2002a: Assimilation of TAO Temperature and TOPEX/Poseidon Altimeter Data into the Poseidon OGCM using a Massively Parallel Ensemble Kalman Filter. Paper presented at the Annual Meeting of the American Meteorological Society, held at Orlando, January 13-17, 2002.

Keppenne, C., and M. Rienecker, 2002b: Initial Testing of a Massively Parallel Ensemble Kalman Filter with the Poseidon Isopycnal Ocean General Circulation Model. *Mon. Wea. Rev*., (in press).

Koster, R. D., M. J. Suarez, and M. Heiser, 2000: Variance and predictability of precipitation at seasonal-to-interannual time scales, *J. Hydromet*., 1(1), 26-46.

Latif M., D. Anderson, T. Barnett, M. Cane, R. Kleeman, A. Leetma, J. O'Brien, A. Rosati, E. Schneider, 1998: A review of the predictability and prediction of ENSO. *J. Geophys. Res*., 103, 14375-14393.

Liou, K. N., 1992: *Radiation and Cloud Processes in the Atmosphere*, Oxford University Press, 487 pp.

Louis, J., M. Tiedtke, J. Geleyn, 1982: A short history of the PBL parameterization at ECMWF, in *Proceedings, ECMWF Workshop on Planetary Boundary Layer Parameterization, Reading, U. K.*, 59-80.

Moorthi, S., and M. J. Suarez, 1992: Relaxed Arakawa-Schubert: A parameterization of moist convection for general circulation models, *Mon. Weather Rev.*, 120, 978-1002.

Reichle, R. H., J. P. Walker, R. D. Koster and P. R. Houser, 2001: Extended vs. Ensemble Kalman Filtering for Land Data Assimilation, submitted to *J. Hydromet*.

Reichle, R. H. and R. D. Koster, 2002: Land data assimilation with the Ensemble Kalman Filter: Assessing model error parameters using innovations, Proceedings of the XIV International Conference on Computational Methods in Water Resources, Delft, Netherlands.

Reynolds R. W., and T. M. Smith, 1995: A high resolution global sea surface temperature climatology. *J. Climate*, 8, 1572-1583.

Sterl, A., and A. Kattenberg, 1994: Embedding a mixed layer model into an ocean general circulation model of the Atlantic: The importance of surface mixing for heat flux and temperature. *J. Geophys. Res*., 99, 14 139-14, 157.

Stevens, B, C.-H. Moeng, and P. P. Sullivan, 1999: Large-eddy simulations of radiatively driven convection: Sensitivities to the representation of small scales. *J. Atmos. Sci.*, 56, 3963–3984.

Stockdale T., 1997: Coupled Ocean-Atmosphere forecasts in the presence of climate drift. *Mon. Weather Rev*., 125, 809-818.

Stull, R., 1989: *An Introduction to Boundary Layer Meteorology*, Dordrecht-Kluwer, 666 pp.

Sud, Y. C., and G. K. Walker, 1999: Microphysics of clouds with the Relaxed Arakawa–Schubert Scheme (McRAS). Part II: Implementation and Performance in GEOS II GCM. *J. Atmos. Sci.*, 56, 3221–3240.

Sundqvist, H., E. Berge, and J. E. Kristjansson, 1989: Condensation and cloud parameterization studies with a mesoscale numerical weather prediction model. *Mon. Wea. Rev.*, 117, 1641–1657.

Tiedtke, M., 1993: Representation of clouds in large-scale models. *Mon. Wea Rev.*, 121, 3040–3061.

Troccoli, A. and K. Haines, 1999: Use of the Temperature-Salinity relation in a data assimilation context, *J. Atmos. Oceanic Technol.*, 16, 2011-2025.

NSIPP Personnel

GSFC Civil Servants
David Adamec (Code 971)
Randy Koster (Code 974)
Michele Rienecker (Code 971)
Siegfried Schubert (Code 910.3)
Max Suarez (Code 913)

Research Scientists
Julio Bacmeister (Code 913, GEST)
Victoria Coles (Code 971, GEST)
Pierre Guillevic (Code 974, GEST)
Christian Keppenne (Code 971, SAIC)
Sarith Mahanama (Code 974, GEST)
Rosana Nieto Ferreira (Code 913, GEST)
Rolf Reichle (Code 974, GEST)
Alberto Troccoli (Code 971, GEST)
Augustin Vintzileos (Code 971, GEST)
Dongliang Yuan (Code 971, GEST)

Research Assistants
Anna Borovikov (Code 971, SAIC)
Michael Kistler (Code 913, SAIC)
Robin Kovach (Code 974, SAIC)
Sonya Miller (Code 971, SAIC)
Philip Pegion (Code 913, SAIC)
Lori Tyahla (Code 974, SAIC)
John Waldrop (Code 971, SAIC)

System Administrator
Richard Mollel (Code 971, SAIC)

Administrative Assistant
Nefertari Johnson (Code 971, SAIC)

<u>NSIPP Publications, 2001</u>

<u>Refereed</u>

Guillevic, P., R. D. Koster, M. J. Suarez, G. J. Collatz, L. Bounoua, and S. O. Los, Influence of vegetation interannual variability on hydrological processes over land surfaces, submitted to *J. Hydromet*.

Herdies, D. H., A. Silva, M. A. F. Silva Dias, and **R. Nieto Ferreira**, The moisture budget of the bimodal pattern of the Summer circulation over South America. *J. Geophys. Res.*, in press.

Keppenne, C., and **M. M. Rienecker**, 2002a: Initial testing of a massively parallel ensemble Kalman filter with the poseidon isopycnal ocean general circulation model. *Mon. Wea. Rev*., (in press).

Keppenne, C. and **M. M. Rienecker**, 2002b: Assimilation of temperature into an isopycnal ocean general circulation model using a parallel ensemble Kalman filter, *J. Marine Systems* (submitted).

Koster, R. D., P. A. Dirmeyer, A. N. Hahmann, R. Ijpelaar, **L. Tyahla**, P. Cox, and **M. J. Suarez**, Comparing the degree of land-atmosphere interaction in four atmospheric general circulation models, *J. Hydromet*., in press.

Koster, R. D., and **M. J. Suarez**, 2001: Soil moisture memory in climate models, *J. Hydromet*., 2, 558-570.

Nieto Ferreira, R., T. M. Rickenbach, D. Herdies, and L. M. V. Carvalho: South American convection organization and circulation patterns during JFM 1998 and JFM 1999. Submitted to the *Monthly Weather Review*, (http://janus.gsfc.nasa.gov/~ferreira/sallj_paper.pdf).

Reichle, R. H., J. P. Walker, **R. D. Koster** and P. R. Houser, 2001: Extended vs. ensemble Kalman filtering for land data assimilation, submitted to *J. Hydromet*.

Rickenbach, T. M., **R. Nieto Ferreira**, J. Halverson, D. Herdies, and M. A. F. Silva Dias, 2001: Modulation of convection in the Southwestern Amazon Basin by extratropical stationary fronts. *J. Geophys. Res.* in press. (http://research.umbc.edu/~rickenba/trmm_lba/Ricken_etal2001.pdf)

Schubert, S., M. Suarez, P. Pegion and **M. Kistler**, 2001: Predictability of zonal means during boreal summer, accepted for publication in *J. Climate.*

Shaman, J., M. Stieglitz, V. Engel, **R. Koster**, and C. Stark: Representation of stormflow and a more responsive water table in a TOPMODEL-based hydrology model, submitted to *Water Resources Research.*

Stieglitz, M., A. Ducharne, **R. D. Koster,** and **M. J. Suarez**, 2001: The impact of detailed snow physics on the simulation of snow cover and subsurface thermodynamics at continental scales, *J. Hydromet*., 2, 228-242.

Sud, Y. C., D. M. Mocko, G. K. Walker, and **R. D. Koster**, 2001: Influence of land-surface fluxes on precipitation: Inferences from simulations performed with ARM-CART SCM dataset, *Mon. Weather Rev*., 14, 3666-3691.

Sui, C. H., X. Li, **M. M. Rienecker**, K. M. Lau, I. Laszlo, and R. T. Pinker, 2002: The impacts of daily surface forcing in the upper ocean over the Tropical Pacific: A numerical study, *J. Clim.,* (in press).

Troccoli, A., M. M. Rienecker, C. L. Keppenne, and G.C. Johnson: Temperature data assimilation with salinity corrections: Validation in the tropical Pacific ocean, 1996-1998, submitted to *J. Geophys. Res*.

Yuan, D., M. M. Rienecker, and P.S. Schopf, 2002: Nonlinear reflection of equatorial Rossby waves at the Pacific western boundary and its role in ENSO, submitted to *J. Geophys. Res*.

Yuan, D., and **M. M. Rienecker**, 2002: Inverse estimation of sea surface heat fluxes over the equatorial Pacific ocean. Part I: Seasonal cycle, submitted to *J. Geophys. Res*.

Non-refereed

Keppenne, C., and **M. Rienecker**, 2001: Design and implementation of a parallel multivariate ensemble Kalman filter for the poseidon ocean general circulation model. NASA Technical Report Series on Global Modeling and Data Assimilation, NASA Tech. Memo-2001-104606, Vol. 21, 35pp (Also http:// nsipp.gsfc.nasa.gov/pubs/tech_rpts/KR_Techmemo2001.pdf).

Keppenne, C., and **M. Rienecker**, 2002: Multivariate assimilation of altimetry into an OGCM with diagnostic sea surface height using the ensemble Kalman filter in Proceedings of the Symposium on Observations, Data Assimilation and Probabilistic Prediction, pp. 158-163, *Amer. Met. Soc*.

Koster, R. D., P. A. Dirmeyer, P. C. D. Milly, and G. L. Russell, 2001: Comparing GCM-generated land surface water budgets using a simple common framework, in Land Surface Hydrology, Meteorology, and Climate: Observations and Modeling, edited by V. Lakshmi, Water Science and Application Volume 3, pp. 95-105, *American Geophysical Union*.

Reichle, R. H. and **R. D. Koster**, 2002: Land data assimilation with the ensemble Kalman filter: Assessing model error parameters using innovations, Proceedings of the XIV International Conference on Computational Methods in Water Resources, Delft, Netherlands.

Schubert, S., M. Suarez, and **P. Pegion**, 2002: Can we predict the next dust bowl? Contribution to the Laboratory for Atmospheres 2002 Annual Report.

Presentations

Keppenne, C., and **M. Rienecker,** Parallel assimilation of altimeter data and in situ temperature data into a quasi isopycnal ocean general circulation model. paper presented at the 26th General Assembly of the European Geophysical Society held at Nice, France, March 26-30, 2001.

Keppenne, C., and **M. Rienecker**, Validation of a parallel ensemble Kalman filter for seasonal-to-interannual forecasting, paper presented at the 2001 Liege Colloquium on Ocean Hydrodynamics held at Liège, Belgium, May 7-11, 2001.

Keppenne, C., and **M. Rienecker**, 2002a: Assimilation of TAO Temperature and TOPEX/Poseidon Altimeter Data into the Poseidon OGCM using a Massively Parallel Ensemble Kalman Filter. paper presented at the Annual Meeting of the American Meteorological Society, held at Orlando, January 13-17, 2002.

Kistler, M., S. Schubert, M. Suarez, and P. Pegion, Predictability of zonal means during boreal summer: A comparison of NSIPP and NCEP models. Climate Diagnostics and Prediction Workshop, La Jolla, CA, Oct 22-26, 2001.

Koster, Randal, Does Soil Moisture Initialization Improve Seasonal Prediction? AGU 2001 Spring Meeting, (Boston, MA), May 2001.

Koster, Randal, Impact of Land Processes on Seasonal Precipitation Forecasts. University of Maryland Dept. of Meteorology Seminar, Oct. 2001.

Koster, Randal, Impact of Soil Moisture Initialization on the Seasonal Prediction of Precipitation and Temperature. GEWEX 4th International Conference, (Paris, France), Sept. 2001.

Koster, Randal, The Continuing Evolution of Land Surface Parameterizations. ECMWF seminar, (Reading, UK), Sept. 2001.

Koster, Randal, The Impact of Land Processes on the Predictability of Precipitation. GFDL seminar, (Princeton, NJ), Feb. 2001.

McLaughlin, D. B., D. Entekhabi and **R. H. Reichle**, Hydrologic Data Assimilation: Challenges and Promising Solutions, Invited Presentation, AGU Spring Meeting, Boston, MA, 2001.

Nieto Ferreira, R. and **M. Suarez,** NSIPP1 Simulations of the SALLJ. Poster presentation at the VAMOS/CLIVAR/WCRP Conference on the South American Low-Level Jet, Santa Cruz, Bolivia, 5-7 February 2002.

Nieto-Ferreira, R. and **M. Suarez**, Two-way interacting regional climate model simulations: predictability of south American precipitation on seasonal to interannual timescales. Oral presentation at the XXVI General Assembly of the European Geophysical Society, Nice, France, 25-30 March 2001.

Nieto Ferreira, R., M. Suarez, R. Koster, T. Rickenbach, and T. Ambrizzi, Two-way interacting regional climate model simulations in the Amazon region. Poster presentation at the NASA/NOAA GAPP Hydrology PIs meeting, Potomac, Maryland, USA, April 30-May-4, 2001.

Nieto Ferreira, R., T. Rickenbach, D. L. Herdies, and L. M. V. Carvalho, Variability of South American convective systems during JFM 1998/1999. Oral presentation at the VAMOS/CLIVAR/WCRP Conference on the South American Low-Level Jet, Santa Cruz, Bolivia, 5-7 February 2002.

Nieto Ferreira, R., T. Rickenbach, D. L. Herdies, M. A. F. Silva Dias, Easterly and westerly wind regimes in Southwestern Amazonia. Oral presentation at the VAMOS/CLIVAR/WCRP Conference on the South American Low-Level Jet, Santa Cruz, Bolivia, 5-7 February 2002.

Pegion, P.J., S.D. Schubert and **M.J. Suarez**, Validation of NSIPP Tier-2 Seasonal Forecasts: What can we gain from improved SST Forecasts? Climate Diagnostics and Prediction Workshop, La Jolla, CA, Oct 22-26, 2001.

Pegion, P.J., S.D. Schubert and **M. J. Suarez,** Validation of NSIPP Tier-2 Seasonal Forecasts: What can we gain from improved SST Forecasts? AMS meeting, Orlando, FL, 13-17 January, 2002.

Pegion, P., M. Suarez, and **S. Schubert**, An analysis of the causes of differences in circulation patterns during the El Niño winters of 1983 and 1998. Climate Diagnostics and Prediction Workshop, La Jolla, CA, Oct 22-26, 2001.

Reichle, R. H., D. B. McLaughlin and D. Entekhabi, Soil Moisture Data Assimilation with the Ensemble Kalman Filter, AGU Spring Meeting, Boston, MA, 2001.

Reichle, R. H., J. P. Walker, **R. D. Koster**, **M. M. Rienecker** and P. R. Houser, Assimilation of soil moisture with the Ensemble Kalman filter in support of NASA's Seasonal-to-Interannual Prediction Project, International Workshop on Catchment-scale Hydrological Modeling and Data Assimilation, Wageningen, Netherlands, 2001.

Reichle, R. H., R. D. Koster, J. P. Walker, **M. M. Rienecker** and P. R. Houser, Aspects of the Extended and Ensemble Kalman filters for land data assimilation in the NASA Seasonal-to-Interannual Prediction Project, Symposium on Observations, Data Assimilation, and Probabilistic Prediction, 82nd AMS Annual Meeting, Orlando, FL, 2002.

Schubert, S., An Overview of Recent Prediction Activities and Data Products of NASA's Seasonal to Interannual Prediction Project (NSIPP). APEC Climate Network (APCN) Working Group Meeting, Seoul, Korea, May 17-18, 2001.

Schubert, **S.,** Global Modeling Activities and NAME. Climate Diagnostics and Prediction Workshop, La Jolla, CA, Oct 22-26, 2001.

Schubert, S., M. Suarez, and **P. Pegion**, Long term drought in the United States Great Plains. Climate of the 20th Century Workshop at COLA, Jan 22-25, 2002.

Schubert, S., M. Suarez, and **P. Pegion**, Predictability of Long term drought in the United States Great Plains. Climate Diagnostics and Prediction Workshop, La Jolla, CA, Oct 22-26, 2001.

Schubert, S., M. Suarez, P. Pegion, and **M. Kistler,** Are droughts in the U.S. Great Plains Predictable on Seasonal and Longer Time Scales? AGU spring meeting, Boston, MA, May 29-June 2, 2001.

Schubert, S., M. Suarez, P. Pegion, and **M. Kistler**, Are droughts in the U.S. Great Plains Predictable on Seasonal and Longer Time Scales? Seminar given at NCEP, June 22, 2001.

Schubert, S., M. Suarez, P. Pegion, and **M. Kistler**, Are droughts in the U.S. Great Plains Predictable on Seasonal and Longer Time Scales? Seminar given at Stony Brook, 2 May, 2001.

Schubert, S, Are droughts Predictable on Seasonal and Longer Time Scales? Laboratory Seminar, 20 February, 2001.

Schubert, S., M. Suarez, P. Pegion, and **M. Kistler**, Decadal Variability in the NSIPP1 AGCM, NASA-IPRC-CLIVAR Workshop on Decadal Climate Variability, January 2001.
Schubert, S.: Predicting Drought in the U.S. Great Plains. Presentation to GEST summer students. 2 August, 2001.

Troccoli, A. and **M. M. Rienecker,** The importance of salinity in the assimilation of temperature observations in the tropical Pacific Ocean, Proceedings of 26th Climate Diagnostics and Prediction Workshop, 2001.

Troccoli, A. and **M. M. Rienecker,** The importance of salinity in the assimilation of temperature observations in the tropical Pacific Ocean, Symposium on Observations, Data Assimilation, and Probabilistic Prediction, 82nd AMS Annual Meeting, 2002.

Yuan, Dongliang, Variational assimilation of satellite sea surface temperature data into the Poseidon quasi-isopycnal ocean model. Seminar at COLA, April 2001.

Yuan, Dongliang, Variational assimilation of satellite sea surface temperature data into the Poseidon quasi-isopycnal ocean model. Presented at the Frontier Research System for Global Change, Tokyo, Japan, February 2001.

Yuan, Dongliang, Inverse estimation of sea surface heat flux over the equatorial Pacific. Poster in WCRP/SCOR Air-Sea flux workshop held in Maryland in May 2001.

NSIPP Science Team

In November 1998 a Science Team of 8 funded collaborations was chosen from a competitive response to an Announcement of Opportunity to collaborate with and support the NSIPP core effort at Goddard. An introductory Science Team Meeting was held in May, 1999. Additional science team members were added from the GMAP NRA in 1999. The second Science team meeting was held July 11-12, 2000 and the third science team meeting June 5-6, 2001. NSIPP also funds collaborations essential to the core effort.

CGCM and AGCM Diagnostics
Grant Branstator, NCAR and M. Chen, Iowa State University, *Diagnosis and simulation of the South-east Asian-induced wavetrain that occurs during tropical Pacific cold and warm events.*

Sumant Nigam, University of Maryland, *Dynamical diagnosis of the NSIPP atmospheric and coupled model simulations*.

John Roads, Scripps Institution of Oceanography, *Seasonal and Atmospheric predictions*.

Chunzai Wang, NOAA/AOML/U. Miami, *Studies of western Pacific Interannual Anomaly patterns toward improved ENSO prediction*.

David Neelin, IGPP, UCLA, *Sensitivity of Precipitation in Coupled Land-Atmosphere models.*

Richard Kleeman, Courant Institute of Mathematical Sciences, NYU, *An investigation of the predictability of the NSIPP forecast system.*

Ping Chang and Ben Giese, TAMU, and R. Saravanan, NCAR, *Modeling Tropical Atlantic Variability*.

Land Surface Model Development and Land Assimilation
Paul Houser, GSFC, and Jay Famiglietti, University of Texas, *Optimal land initialization for seasonal climate predictions*.

Ocean data assimilation and coupled forecasting
Eugenia Kalnay, University of Maryland, *Ensemble ocean-atmosphere perturbations with growing ENSO modes using breeding*.

Thorsten Markus, JCET/GSFC/UMBC, *Improved Surface Heat and Salt Fluxes at polar latitudes through the assimilation of satellite measurements.*

Ocean Model Development
William Dewar, Florida State University, *Thermodynamics in layered models*.

NSIPP Associate Investigators

Paul Schopf, George Mason University, *Development of the Poseidon Ocean Model for NSIPP*.

Marc Stieglitz, Lamont Doherty Earth Observatory, *Land surface model development for NSIPP*.